CROSS-TALK ANALYSIS OF A 12 CHANNEL 2.5 GB/S VCSEL ARRAY BASED PARALLEL OPTICAL INTERCONNECT FOR A MULTI-STAGE SCALABLE ROUTER ARCHITECTURE

PATRICK ARSENAULT

Department of Electrical and Computer Engineering
McGill University
Montreal, Canada
March 2002

A thesis submitted to the Faculty of Graduate Studies and Research in partial fulfillment of the requirements of the degree of Master of Engineering

Your file Votre référence
ISBN: 0-612-88700-6
Our file Notre référence
ISBN: 0-612-88700-6

ABSTRACT

To support and keep pace with the Internet growth, new routers based on optical multi-stage architectures are emerging. These routers consist of multiple shelves interconnected with parallel optical interconnects. This thesis proposes the analysis of the inter-channel crosstalk of a state-of-the-art 1x12 VCSEL and PIN array based parallel optical interconnect operating at 2.5 Gb/s. The crosstalk properties of the parallel optical interconnect will impact the optical power link budget and scalability of these multi-stage routers.

To study the crosstalk properties of the optical interconnect, a special test set-up and detailed test procedures were created to analyse the bit error rate and jitter performance of the parallel optical interconnect in multi-channel operation. The results obtained from the pre-defined experiments confirmed the degradation of the interconnect performance due to inter-channel crosstalk. This performance penalty also limits system scalability, especially when it is combined with the inherent crosstalk properties of the optical redirection boxes. The sources of inter-channel crosstalk were also determined. Finally the system optical link budgets were adjusted and rough system scalability limits were obtained.

SOMMAIRE

Pour supporter l'évolution rapide de l'Internet, une nouvelle forme de routeur basé sur une architecture multi-stages est sur le point d'émerger. Ces routeurs sont composés de plusieurs châssis interconnectés au moyen de systèmes à base d'optique parallèle. La présente thèse propose une analyse de diaphonie (« crosstalk») inter-canaux d'un système d'interconnections optiques parallèles basé sur une technologie de pointe consistée de 1x12 VCSEL et PIN fonctionnant à 2.5 Gb/s. Les propriétés de diaphonie du système d'interconnections à optique parallèle vont affecter l'expansibilité de ces routeurs à base d'architecture multi-stages.

Pour étudier les propriétés de diaphonie de ces composantes optiques, un appareillage spécial ainsi que des procédures de tests détaillées ont été faites pour déterminer la différence du taux d'erreurs sur les bits ainsi que la variation de la performance des canaux optiques quand tous les canaux fonctionnent simultanément. Ceci a permis l'analyse de l'impact de la diaphonie inter-canaux sur la performance du système et son expansibilité. Les résultats obtenus quand les tests prédéfinis ont été exécutés ont confirmé qu'une dégradation de performance est causée par la diaphonie inter-canaux. Cette dégradation de performance quand elle est combinée à la diaphonie des boites d'interconnections optiques peut limiter l'expansibilité d'un système. Les sources de diaphonie inter-canaux ont aussi été déterminées. Pour conclure, les budgets de puissance de liens optiques pour systèmes à architecture multi-stages ont été déterminés et rajustés basé sur les résultats obtenus lors de cette expérimentation et les limites approximatives de l'expansibilité de tels systèmes ont aussi été évaluées.

ACKNOWLEDGEMENTS

Firstly, I would like to thank David Plant, Andy Kirk and Professor M. L. Blostein for their kind guidance and support at the start of my project and for believing in "this" mechanical engineer who came out of nowhere with the crazy idea of becoming an electrical engineer. I would also like to express my sincere and deepest gratitude to Lawrence Chen who took over from David as my supervisor with no question asked and offered great advice, encouragement/support throughout the development and completion of this thesis.

I would also like to thank all the grad students for their patience and teaching, and especially Robert Varano, for his invaluable help in the McGill lab, as well as Mike Ayliffe, Fred Lacroix, Mike Venditti and David Rolston for their patience in helping me understand some of the theory behind this "optical stuff". I would like to thank my colleagues at McGill and especially Mitch Salzberg and the rest of the CITR team for all their kind help.

I would also very much like to express my gratitude to the Photonics Team at Hyperchip. Without them, it would have been impossible to complete this thesis. A special thank you goes out to Nicolas Berlinger, Nicolas Villeneuve, Ozzy Mermut, Francois Castonguay, Simon Gosselin and Mitch Salzberg as without their help and testing insights, I would never have been able to complete this thesis. I also want to thank the Photonics Group manager, Francois Guevin, for giving me access to the photonics lab and resources. I would especially like to thank Carle Beauchamp for creating such a dynamic team and for picking such cool people to work with. I also would like to thank the IPR group at Hyperchip, i.e. David Chamberlain, Marc Benoit, Ann Lamarche and Lea Hardcastle. I wish to express my gratitude to Hyperchip Inc. for supporting this activity.

Finally I would like to thank my cherished daughters Emmanuelle and Chloé, and my dear wife Isabelle who always dealt with my long hours with a smile and encouraging words. Their inspiration drove me to finish this thesis and I could never have done it without their support.

To Isabelle, Emmanuelle and Chloé, with all my gratitude.

TABLE OF CONTENTS

LIST OF TABLES

LIST OF FIGURES

Chapter 1

Introduction

To support Internet growth, a new generation of routers based on multi-stage interconnect networks (MIN) is emerging. These are driving the introduction of cost effective high-bandwidth optical interconnect technologies. However, one significant factor limiting system performance and scalability is the crosstalk induced in parallel optical interconnects (POI). This thesis is concerned with investigating the impact of POI crosstalk on system performance. An outline of the following chapters is presented at the end of this chapter.

1.1 Internet Network Growth and System Scalability

1.1.1 Network Growth

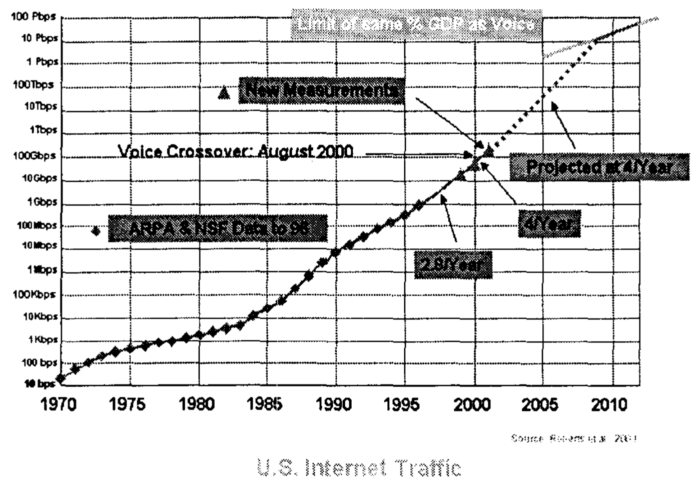

Figure 1: U.S. Internet traffic growth [2]

Internet traffic is projected to grow at more than 100% per year [1] while Internet backbone capacity is doubling every 6 months as shown in Figure 1[2]. Actual growth figures vary from study to study [3, 4, 5, 6, 7], but they all point to the fact that very large routers will be needed to support next generation IP networks.

1.1.2 Router Scalability

Routers are the building blocks of today's Internet infrastructure and are typically segmented in many different layers, one of which is the "core" router layer. Core routers in general aggregate the traffic coming from the customer facing edge routers. They typically support very high Internet traffic throughput, and act as gateways to the optical backbone networks "where traffic volumes and cost of failures are the highest" [1].

Most of the core routers deployed in today's telecom networks are limited in terms of port count and can support a maximum of 8 to 15 OC-192 interfaces [8, 9]. With the IP bandwidth growth shown in section 1.1.1, core routers are expected to reach their capacity limits in the near future [1]. Using expensive revenue-generating interface ports to interconnect many routers together is the only way to scale today's router. This represents a costly solution for cost-sensitive service providers (on average approximately $250 K US per OC-192 port) [10]. Furthermore it results in the additional drawback of reducing the total number of revenue generating ports per system.

To meet today's network growth requirements, a new breed of scalable routers or "super-routers" [1] is needed. They will support a large numbers of interface ports and will use switch fabric interconnections in a cost-effective and efficient manner.

1.1.3 Multi-Stage Architecture and the Need for Optical Interconnect

This new type of scalable router architecture is similar to the multi-stage interconnect networking (MIN) architectures found in the computer industry. It consists of interconnecting the switch fabric of many shelves together as shown in Figure 2. This architecture maximizes the use of revenue generating interface ports. Some new scalable core router architectures are already found commercially and provide between 5.12 Tb/s and even 19.2 Tb/s of aggregate capacity. Three main topologies are used: Multi-Stage [11], Thoroïdal Mesh [12] or Hypercube [13].

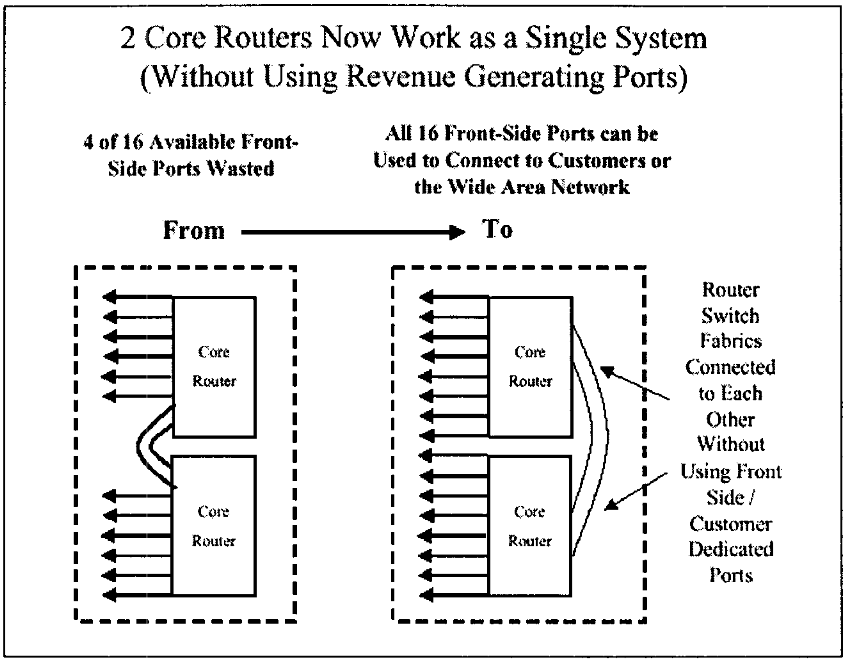

Figure 2: Scalable router architecture based on switch fabric interconnection [1]

These new multi-chassis architectures require an interconnect scheme with the following attributes:

- cost efficiency and reliability
- high bit rate support (> 2.5 Gb/s)
- high aggregate capacity (>10 Gb/s).
- low footprint
- capability to support various interconnection lengths (at least several hundred meters)

Optical interconnects have been shown to offer many advantages over electrical connections for "shelf-to-shelf " or "inter-shelf" applications [14, 15]. For scalable router applications, 850 nm VCSEL based parallel optical technology is best suited (this will be discussed in Chapter 2) and offers the added capability for increasing the interconnect distance to several hundred meters. Even though the technology has been confined to laboratory demonstrations for many years, commercial VCSEL array based parallel optical technology, for example 4 or 12x2.5 Gb/s channel technology is currently emerging [16, 17, 18, 19].

VCSEL technology also provides a solid platform upon which next generation components that further increase interconnect bandwidth capacity can be based. As routers scale to larger systems, ultra compact highly dense components will be needed. Already, components supporting 32x2.5 Gb/s channels have been reported [20, 21, 22]. WDM based VCSEL array technology also offers interesting interconnect alternatives [23, 24].

1.1.4 New MIN Architecture

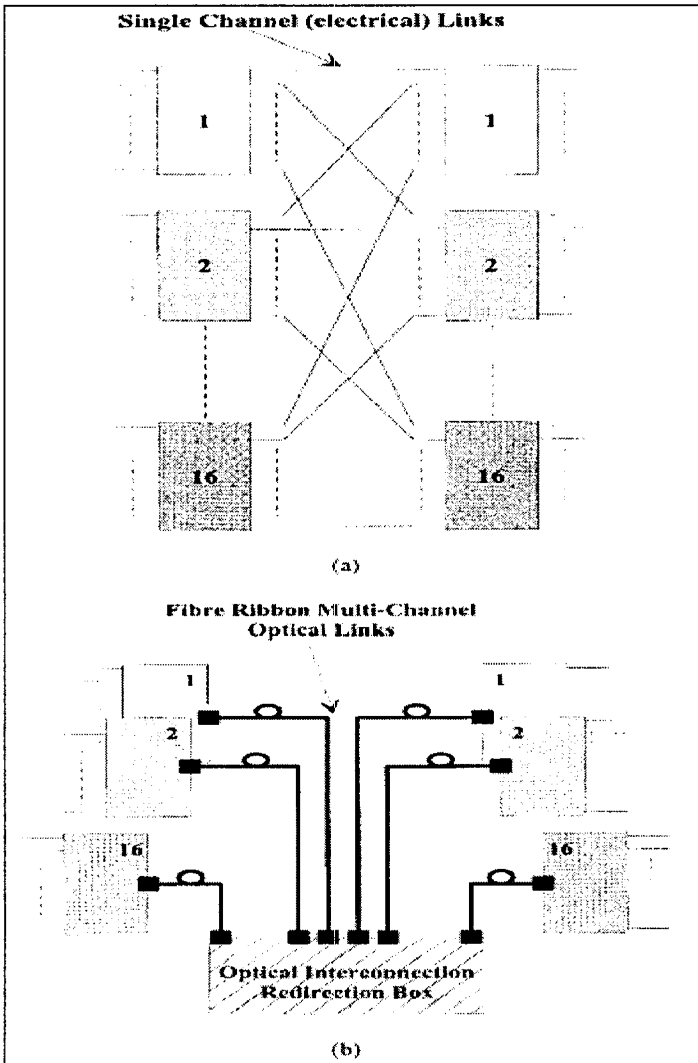

Figure 3: O-MIN architecture with optical redirection box [25]

Router architectures that scale using optical interconnect links can be viewed as optical MINs or O-MINs. Scaling O-MINs increases system complexity and cost since optical interconnect technology is expensive in general.

An optical interconnection or redirection box (RB), composed of passive or active optical technology, will simplify the O-MIN interconnection scheme and reduce the total number of expensive optical-to-electrical-to optical (OEO) conversions [25]. Figure 3b shows an example of an O-MIN using an optical redirection box instead of the electrical connections (depicted in Figure 3a). All-optical O-MINs are not practical with today's optical technology but hybrid O-MINs, which use a form of circuit switching at the optical layer to minimize OEO processing, will appear in the near future [26, 27]. In fact, component vendors are already touting the use of low-cost electrical switches with parallel optical technology (POI) technology [28, 29].

1.1.5 Scalability Limitations of Optical MINs

To scale O-MINs further, many optical interconnection boxes can be connected together. Figure 4 shows an example of such a scaled O-MIN architecture. It is well known that optical crosstalk characteristics of the redirection boxes will limit system performance and consequently its scalability [30, 31, 32]. Figure 4 also identifies possible sources of crosstalk. POI crosstalk can occur at the transmit end and receive ends of the POI, and is also an inherent component of the redirection box itself.

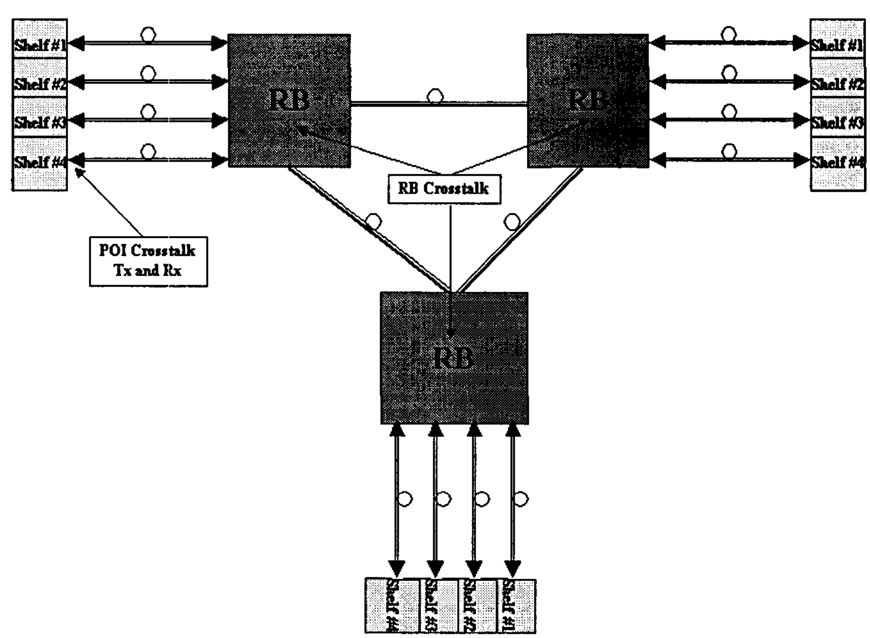

Figure 4: Scalable O-MIN architecture

The crosstalk, and more specifically the optical crosstalk inherent to the POI technology, will be one of the primary limitations on system performance and scalability.

Inter-channel crosstalk within the POI will impose a power penalty over single channel operation of the POI. This will degrade the system's optical link budgets of a scalable O-MIN architecture [24]. Crosstalk will also degrade the jitter performance of the optical POI links [29].

Optical crosstalk within the POI links can limit the total number of optical redirection boxes that can be interconnected to scale an O-MIN. Although several new MIN architectures have been proposed to minimize the impact of crosstalk on O-MIN performance [26, 27], the crosstalk performance of POI links will nevertheless impose additional crosstalk requirements on the optical redirection technology used in today's O-MINs.

1.1.6 Network Implementation Considerations

System reliability and cost are two of the most important criteria considered by service providers when purchasing new routing equipment for their network [7, 33]. These two items will represent key attributes, which will affect technological choices.

1.1.6.1 The Carrier-Class Reliability Paradigm

Optical interconnect components used in telecom grade networking equipment have to be robust and reliable enough to enable the system to meet "carrier-class" system reliability standards. In general, this requirement means 99.999% system availability, or approximately 5 minutes of down time per system per year over the lifespan of the system [34].

To meet these system level reliability targets, component reliability targets are even more stringent. These have barely changed since 1992 as described in [35, 36] for a generic switching central office environment. One criteria of importance for the work in this thesis is:

- $BER_{DATA} < 10^{-14}$ (the bit error rate is maintained below 10^{-14} for 1 Gb/s data rates)

1.1.6.2 Cost Sensitivity

The highly competitive environment and tightening capital budgets are forcing service providers to push further the equipment vendors for dramatic price reduction in equipment. Tenfold price reduction is expected for systems in the next year. With optical components representing one of the major router cost component [1, 5], they will be under constant price reduction pressure.

1.2 Thesis Outline and Organization

1.2.1 Project scope and Challenges

The work presented in this thesis is part of a series of studies undertaken at Hyperchip to characterize commercially available POI technologies. A detailed understanding of POI properties is essential in order to implement state-of-the art POI technology in core router applications. It is complementary to the work done in [37], which characterizes the performance of the POI components used in scalable router designs and is essential for understanding the scalability of scalable router architectures using POI technology.

The objective of this thesis is to characterize the impact of optical and electrical crosstalk on the performance of a 12x2.5 Gb/s channel POI used in an O-MIN router architecture. The work done in this thesis focuses on defining the power penalty and jitter budget penalty due to crosstalk and in particular, determining the optical crosstalk, which can affect the scalability of multi-stage scalable routers. We confine our study to a state-of-the art 12x2.5 Gb/s POI from Agilent Technologies. Nevertheless, the methodology and characterization process provide a general framework for analyzing the crosstalk performance of other POI technologies and identify key selection criteria for evaluating POI technology used in telecom applications.

Several challenges presented themselves throughout the completion of this thesis: Dealing with state-of-the art technology created component availability and reliability issues. Testing equipment availability and price was also an issue. Finally, dealing with sensitive, i.e. proprietary, and confidential information from component vendors represented a last challenge.

1.2.2 Thesis Organization

Chapter 2 provides a general description of the POI components used in this thesis and the reasons for their selection. An overview of the sources of crosstalk is provided in Chapter 3, as well as key techniques used for minimizing crosstalk. This information will be used when selecting other POI components for testing.

Chapter 4 explains the impact of crosstalk on POI performance as well as the implications on system performance and scalability. The experimental set-up and procedure specifically designed to measure crosstalk and the associated performance penalties, are described in Chapter 5. Tests used during experimentation have been carefully selected to identify the possible sources of POI crosstalk. Test results are shown in Chapter 6 and an analysis of the impact of crosstalk on POI and system performance is provided. Finally, concluding remarks and future topics for investigation are given in Chapter 7.

1.3 References

1. Steve Kamman, James Moon,"Core Routers: The Dilithium Crystals of the Internet", CIBC World Markets Equity Research, December 12th 2001.

2. Caspian Networks, "US Internet IP Traffic Growth", Webcast Presentation, August 2001. http://www.caspian.com/pressroom/press/08.15.01.shtml

3. TeleGeography 2001, "Global Telecommunications Traffic Statistics and Commentary", TeleGeography Inc., Washington DC, USA, 2001.

4. Michael E. Ching, Samuel Wilson, "Data Networking IP Switching & Routing: Making the Net Work 1.0", Merrill Lynch, 13th February 2001.

5. Steve Kamman, "Networking Market Research: Disruptive Change In The Network Means Disruptive Change In Network Equipment", CIBC World Markets, Equity Research, January 9th 2001.

6. C. Armacost, M. Jung, A. Michon, "Data Networking Industry Perspectives", SG Cowen Market Report, May 2001.

7. Infonetics Research, "The Service Provider Opportunity in Europe 2000: Alternative Carrier", San Jose California, September 2000.

8. Juniper Networks, "M160 Internet Backbone Router", Product Data Sheet, USA, 2000. http://www.juniper.net/products/dsheet/100012.html#07

9. Cisco Systems, "Cisco 12416 Internet Router", Product Data Sheet, USA, 2001. http://www.cisco.com/warp/public/cc/pd/rt/12000/

10. Light Reading, "Internet Core Router Test", Test Results, USA, March 2001. http://www.lightreading.com/document.asp?doc_id=4009

11. Charlotte's Web Networks, "Aranea 1 Terabit Router", Product Data Sheet, 2001. www.cwnt.com/product.htm

12. Avici Systems, "The Avici TSR™ Scalable Core Router", Product Brochure, USA, 2001. http://www.avici.com/documentation/datasheets/Avici_TSR.pdf

13. Pluris, "Teraplex^{TM} 20 Internet Core Router", Product Data Sheet, USA, 2001. http://www.pluris.com/products/teraplex20/index.cfm

14. Christopher Tocci, John Caulfield, "*Optical Interconnection, Foundation and Applications*", Artech House, Boston USA, 1994.

15. C.M. Ryu, U. Koelle, S.R. Johnson, P.Dowd, R. Turoin, P. Kelkar, and Y. -H. Zhang, "Optical interconnects for high-speed data links, SPIE Conference on Optoelectronics Integrated Circuits III, SPIE Vol. 3631, San Jose, California, January 1999.

16. Alvesta, "3100 Series Optical Tranceivers", Product Data Sheet, 2001. http://www.alvesta.com/products.html

17. Zarlink Semiconductors, "MFT62340 12-channel Transmitter - 2.5Gb/s per channel", Product Data Sheet, 2001. http://products.zarlink.com/partfinder/prodprofile.cgi?device=1007&path=products/product_finder/group:23

18. Picolight, "30 Gb/s Parallel Optical Interconnect", Product Data Sheet, 2001. http://www.picolight.com/products/30gbspoi.html

19. Agilent Technologies," 30 GBd Fiber-Optic Link for High-Volume, Short-Range Applications", Product Data Sheet, 2001. http://www.semiconductor.agilent.com/cgi-bin/morpheus/promotions/promotionsDetail.jsp?promoID=20163

20. F. Mederer, R. Michalzik, K. J. Ebeling, "High-speed parallel optical interconnects based on vertical cavity surface emitting lasers", Compound Semiconductor 6(5) July 2000.

21. Y. -M. Wong, D. Muehlner et al., "Technology Development of a High-Density 32-Channel 16 Gb/s Optical Data Link for Optical Interconnection Applications for the Optoelectronic Technology Consortium", Journal of Lightwave Tech., Vol. 13, No. 6, June 1995.

22. Xanoptix, "XTM-72, Next-Generation Optical Connections", Product Brochure, USA, 2001. http://www.xanoptix.com/xtm-72.pdf

23. L. A. Bergman, C. Yeh, J. Morookian, "Advances in Multi-Channel Optical Multi-Gbytes/sec. Bit-Parallel WDM Single Fiber Link", 50th Electronic Components & Technology Conference, 2000, Conference Proceedings. USA, 2000.

24. M.C. Larson, M.D. Pocha, et al., "Multiwavelength VCSEL Transmitter for WDM Parallel Optical Fiber Interconnects", 12th Annual Meeting IEEE Lasers and Electro-Optics Society (LEOS 1999), Conference Proceedings, vol.2, San Francisco, USA, Nov. 1999.

25. Bostica, M. Burzio, F. Delpanio, P. Pellegrino, L. Pesando, "Ten-Channel Optical Transmitter Module for Sub-System Interconnection Operating at $\lambda = 1.3$ μm up to 12.5 Gbit/s", IEEE Transactions on Advanced Packaging, Vol. 22, No. 3, August 1999.

26. Y. Pan, C. Qiao, Y. Yang, "Optical Multistage Interconnection Networks: New Challenges and Approaches", IEEE Communications Magazine, February 1999.

27. Y. Yang, J. Wang, Y. Pan, "Permutation Capability of Optical Multistage Interconnection Networks", Parallel Processing Symposium, Orlando, USA, April 1998.

28. L.A. Buckman, K.S. Giboney, et al.,"Parallel Optical Interconnect", Lasers and Electro-Optics, CLEO 2000 Conference Proceedings, San Francisco, USA, May 2000.

29. K. Droggemuller et al., "Current Progress of Advanced High Speed Parallel Optical Links for Computer Clusters and Switching Systems", Proceedings IEEE Electronic Components and Technology Conference, 2000.

30. L. Gillner, C. P. Larsen, M. Gustavsson, "Scalability of Optical Multiwavelength Switching Networks: Crosstalk Analysis", Journal of Lightwave Technology, Vol. 17, No. 1, Jun. 1999.

31. E.L. Goldstein et al.,"Performance Implication of Component Crosstalk in Transparent Lightwave Networks", IEEE Photon. Tech. Lett., Vol. 6, No. 5, May 1994.

32. L. Gillner, C. P. Larsen, M. Gustavsson, "Statistical Analysis of Inteferometric Crosstalk: Theory and Optical Network Example", Journal of Lightwave Technology, Vol. 15, No. 11, Nov. 1997.

33. Infonetics Research, "The Service Provider Opportunity in North America: Tier 1 Carriers", San Jose California, September 2000.

34. Telcordia Technologies, "GR-418-CORE - Generic Reliability Assurance Requirements for Fiber Optic Transport Systems ", Issue 2, December 1999.

35. R.A. Nordin, A.J.F. Levi, et al., "A System Perspective on Digital Interconnection Technology", Journal of Lightwave Tech., Vol. 10, No. 6, June 1992.

36. M. Niburg, P. Eriksen, K. Gustafsson et al, "A Complete Sub-System of Parallel Optical Interconnects for Telecom Applications", Proc. Electronic Components and Technology Conference, 2000.

37. M. Salzberg, "Testing and Characterization of a Parallel Optical Interconnect for a Scalable Routing System", Master's thesis, McGill University, 2001.

38. M. Grammatikakis, D. F. Hsu, M. Kraetzl, *"Parallel System Interconnections and Communications"*, CRC Press LLC, Boca Raton, USA, 2001.

Chapter 2 Technological Considerations and Description of the Experimental Optical Interconnect

The optical technology best suited for short distance high bandwidth optical interconnects in scalable router applications is based on 850 nm vertical cavity surface emitting laser and p-i-n (VCSEL/PIN) arrays as will be explained in the first portion of this chapter. The POI components used in this paper are all commercially available parts. Key component characteristics affecting crosstalk performance will be described in the second part of this chapter.

2.1 Advantages of VCSEL/PIN Array based POI

As stated in Chapter 1, MINs require a shelf-to-shelf interconnect solution providing as much bandwidth as possible over a distance of several hundred meters. Telecom-grade MINs impose the additional requirements of density, power consumption as well as reliability and cost-effectiveness.

References [1, 2] detail the advantages of parallel optical technology over electronics for inter-shelf communications in a carrier-class switching environment. In summary, as data rates increase to speeds greater than 400 Mb/s, electrical interconnects are limited by, distance (conductor and dielectric loss), cross- talk, power and pin-out density [3, 4].

Of all the short wavelength lasers used for short distance applications, 850 nm based VCSELs (typically InGaAS/GaAs based lasers) are best suited. In particular, they offer performance improvements over other technologies: low threshold current, high efficiency, relative temperature independence, multi-mode emission properties, as well as the ease with which they can be driven (see Figure 5 [5] and Table 1 [5]).

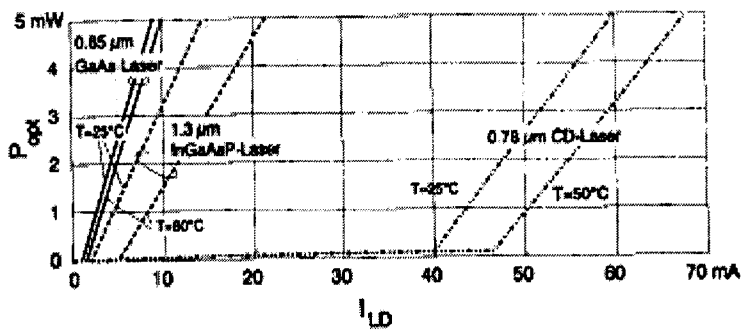

Figure 5: Graph of optical power versus diode current for 3 different laser diodes [5]

TABLE I

COMPARISON OF PROPERTIES OF LASER DIODES WITH DIFFERENT WAVELENGTHS FOR OPTICAL INTERCONNECTIONS

λ (μm)	I_{th}	T_o	f_{3dB}	MM-prop.	Reliability	Driving Ease	Eye Safety
0.78	--	o	-	++	-	-	o
0.85	++	+	+	+	+	++	o
1.3	+	--	+	o	+	o	+
1.55	+	--	+	-	+	-	++

Table 1: Comparison of different laser diode properties [5]

Other features of 850 nm VCSEL based technology include lowers module costs through simplified packaging [6], standard testing techniques and a minimum of monitoring circuits. Furthermore, combining 850 nm VCSELs with large core size multi-mode fiber relaxes the alignment constraints between the laser/photodiodes, and standard IC fabrication techniques, testing and mounting technologies have already been proven for mass production. Finally, 850 nm VCSEL technology is becoming somewhat of a commodity [7] and is thus inexpensive.

Advances in 1-D VCSEL/PIN array based POI technology [8, 9, 10, 11, 12, 13] have just recently been translated into commercial high-bandwidth optical interconnect products. Today, only a few vendors provide VCSEL/PIN array-based components, such as Agilent, Zarlink, Picolight, and Alvesta, to name a few, [14, 15, 16, 17]. As stated in Chapter 1, such technology meets the requirements for multi-stage scalable router architectures. A further advantage of 850 nm VCSEL arrays is the uniform performance of its elements across the arrays. This can provide further cost reduction as it either simplifies or completely removes the need for laser monitoring circuits. Such technology is gaining widespread acceptance as demonstrated by its increasing promotion at industry forums such as the Optical Internetworking Forum (OIF) [18].

The relative advantages of VCSEL based arrays over other optical technologies available today are shown in Table 2. A "++" sign identifies the components having a distinct advantage over other technologies listed in the table.

	Bandwidth	**Relative Footprint**	**Power Consumption**	**Relative Cost Factor (Price/Gb)**	**Transmission Distance**
Typical TDM Edge Emitters 1310-1550 nm [19,20]	10 Gb/s (40 Gb/s)	-- --	- - --	- - ---	+ + +
TDM VCSELs [16]	10 Gb/s	-	+	+	+
CWDM [21]	10 Gb/s	+	++	+	+
VCSEL Arrays 850 nm [14, 15, 17, 22, 23]	10 Gb/s, 30 Gb/s, 90 Gb/s, 120 Gb/s	++	+	+ +	- -

Table 2: Comparison of optical technology used for high bandwidth interconnect applications

In terms of bandwidth capacity, VCSEL/PIN array-based POIs are already offering aggregate bandwidths of 30 Gb/s. TDM technology based on conventional edge emitting devices does maximize bandwidth within a single fiber link but typically occupies more board space than VCSEL based technology on a gigabit per square millimeter basis. They also require additional multiplexing and demultiplexing circuitry, which increases the total board footprint of the TDM solution. New VCSEL based TDM technology does offer a board space improvement [16]. However, TDM applications dissipate more power than VCSEL based POI technology on a per gigabit basis, especially when the power requirements of the additional circuitry are factored in. Thus, in terms of cost per gigabit of transmitted bandwidth, VCSEL based POI is more cost effective. The transmission distance of VCSEL based POI is limited to a few hundred meters which does not represent a problem for O-MIN architecture applications described in this thesis.

VCSEL array based POI technology provides a simple roadmap for increased bandwidth capacity. Increasing the array size or modulation frequency can easily increase the aggregate bandwidth. Such new components will be needed as O-MINs scale to the system sizes described in Chapter 1 or even larger.

The ability to scale current VCSEL/PIN array based POI technology is promising. Prototypes of components operating at 36x2.5 Gb/s (or 90 Gb/s of aggregate capacity) and even 48x2.5 Gb/s (or 120 Gb/s of aggregate capacity) [22, 23] have been demonstrated. Operation of a 16x16 VCSEL array operating at 1 Gb/s (256 Gb/s) has also been shown in a laboratory experiment [24]. Increasing the data transmission speed of current 2.5 Gb/s links can also provide more bandwidth: high speed VCSELs operating at rates of up to 10 Gb/s and 12.5 Gb/s have been reported [25, 26]. However the need for further scaling of POI technology is not foreseen in the immediate future.

Combining VCSEL technology with WDM technology, offers an interesting approach for increasing bandwidth while providing the added advantage of reducing the total fiber count of POI links used in O-MIN architectures. Already, experiments of POI links have shown 4x2.5 Gb/s and 4x10 Gb/s Coarse Wavelength Division Multiplexing (CWDM) channels in operation [7, 26, 27]. Even a 100 Gb/s solution based on CWDM has been demonstrated [21] showing the great potential of the combination of CWDM and VCSEL/PIN array technologies.

2.2 Disadvantages of 850 nm POI technology

One of the issues impacting the performance of VCSEL/PIN array based POI links is crosstalk, and more specifically electrical and optical crosstalk. Several techniques developed to mitigate component crosstalk in POI will be discussed in the next chapter. As the POI components scale to larger arrays and provide higher bandwidth, crosstalk can become more of a limiting factor.

A second disadvantage of 850 nm POI technology is reliability, especially that of 1-D VCSEL/PIN array based technology, which still needs to be proven. To date, because of their limited deployment in telecom networks, there is little reliability data available for POI. Many vendors are working to obtain such data through repeated testing [29]. Only long periods of utilization will provide accurate reliability numbers. However it is expected that reliability of VCSEL/PIN array based POI will improve over time especially since their manufacturing process is based on standard silicon fabrication technology. Additionally, using strained InGaAs quantum wells improves the overall lifetime of the VCSELs [5]. Although the reliability of 2-D array technology is expected to be worse than for 1-D array components ([25] shows a decrease in manufacturing yields with the increase in array sizes), improvements are expected once these devices are mass-produced. There are also encouraging signs demonstrating improvements in the reliability of POI technology: [30] demonstrated carrier-class operation of a 10x1.25 Gb/s channel POI which maintained a BER figure of 10^{-14} with a power budget of 10 dB and a small power consumption of 130 mW per channel.

POI require multiple fiber terminations but evolving standard multi-fiber ribbon connectors such as the MTP™ and their termination process alleviate this problem. A final disadvantage is the use of standard multimode fibers used in POI, which are not suited to transmit at high data rates over long distances. Typical transmission distances over multimode fiber are less than 300 meters; however with special index profile MMF, transmission distances can be improved and distances greater than 400 meters have been reported at 12.5 Gb/s [25].

2.3 Experimental POI Description

The POI studied in this thesis has already been described in detail in [31] and only features pertinent to the crosstalk study undertaken this thesis will be presented below. This description provides information complementary to that provided in [31]. Further details can be obtained from the component manufacturer's datasheets themselves. Note that only off-the-shelf or commercially available components were used in this experiment. For this first study, the component suppliers selected were picked at random from a number of commercially available VCSEL/PIN array based modules all offering high aggregate bandwidth (30 Gb/s), low power consumption and small footprint (Alvesta, Picolight and Agilent) [15, 16, 17].

2.3.1 General Diagram

The experimental POI consists of twelve 2.5 Gb/s channel VCSEL/PIN array based transmitter/receiver modules. Coupling to standard 62.5 μm multi-mode ribbon fiber (MMF) is achieved with standard 12 channel MTP™ connectors, which come integrated in the transmitter (Tx) and receiver module (Rx). This is illustrated in Figure 6.

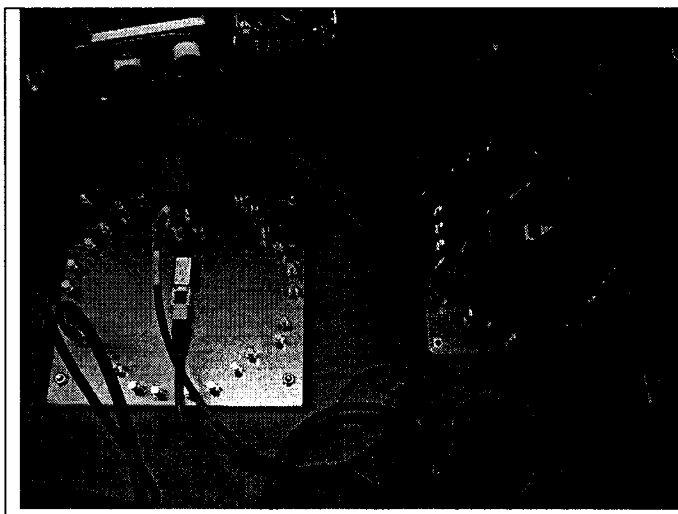

Figure 6: Experimental transmitter (right) and receiver (left) modules mounted on test boards interconnected with a 12-channel multi-mode fiber ribbon cable.

2.3.2 The Transmitter Module (Tx):

The Tx module is based on 12x2.5 Gb/s channels using 850 nm oxide-confined InGaAsP multi-quantum well (MQW) VCSEL array made by Agilent (part # HFBR-712BP) [32]. It is integrated with a custom 12 channel laser driver IC and operates from a single 3.3 V power supply. It provides low-voltage transistor-transistor logic (LVTTL) and low-voltage complementary metal oxide semiconductor (LVCMOS) control interfaces and current mode logic (CML) compatible data interfaces. It comes with an integrated standard MTP™ (MPO) connector. Finally, electrical connections of the Tx module are ball grid array (BGA) based which render inaccessible the module pins to external probing which will be seen later when testing the components in Chapter 5. The average optical output power varies between –8 and –3 dBm while the extinction ration (ER) varies between 5 and 6 dB [32]. This wide variation indicates that optical output power variation across the VCSEL array will have to be characterized at the start of the experimentation. RIN is specified at – 124 dB/Hz, which is low enough (< -112 dB/Hz) for the POI applications considered in this thesis [33, 34].

2.3.3 The Receiver Module (Rx):

The corresponding 12-channel PIN photodiode array is also from Agilent (part number HFBR-722BP) [32]. It is coupled with an integrated pre/post amplifier integrated circuit and like the Tx module described above, it operates from a single 3.3 V power supply. It provides LVTTL and LVCMOS control interfaces and CML compatible data interfaces. It is integrated with a standard MTP™ (MPO) connector and the electrical connections are also BGA based. Minimum receiver sensitivity is specified at – 16 dBm. This value will be useful when measuring POI bit error rate (BER) with variations in input optical power.

2.3.4 Fiber Characteristics

FiberExpress 62.5 μm/125 μm graded-index multi-mode fiber ribbon (MMF) from Nordx/CDT was used [35]. It was connectorized with standard MTP™ connectors. The key characteristics of the fiber ribbon are listed below:

- 3.25 dB/km attenuation
- 200 MHz*km bandwidth
- 0.2 numerical aperture
- zero crosstalk between channels due to cladding confinement and channel separation (specified by the fiber ribbon supplier) [36]

2.3.5 Optical connectors:

The key attributes of the standard MTP™ connectors provided on both the Tx and Rx modules as well as the fiber ribbon cable are specified below [37]:

- 0.2 dB typical over all fibers (0.50 dB maximum); the performance across the array is expected to be uniform at the connectors
- <0.2 dB difference over 1000 mate/unmate cycles (this shows that frequent manipulation of connectors will not cause a large variation in experimental results)
- 125 μm pitch between channels

2.3.6 Test board characteristics.:

The VCSEL and PIN array modules were mounted on test boards supplied by the component vendors (HFBR-7001 and HFBR-7002) [38, 39]. The wire lengths for each channel were verified by examining the Gerber files of the test boards, which were graciously provided by the supplier [40, 41]. The wire lengths were equal for all channels on the test boards (± 250 μm).

2.4 Summary

In this chapter, we considered the use of an 850 nm VCSEL/PIN array based POI. They represent state-of-the-art technology and provide the most cost-effective technology available for high-bandwidth interconnect in telecom-grade scalable O-MIN architectures. The POI used in this experiment is composed of commercially available components only. This minimizes the inherent risks associated with the unknown reliability of VCSEL/PIN based array technology. The technologies are based on the proven silicon mass fabrication process, which mitigates such risks: when the VCSEL array vendors will produce large numbers of these components, their reliability should improve. Additional specifications pertaining to the crosstalk characterization are also provided.

2.5 References

1. R. A. Nordin, D. B. Buchholz, et al., "High Performance Optical Datalink Array Technology", IEEE Transactions on Components, Hybrids, and Manufacturing Technology, Vol. 16, No. 8, Dec. 1993.

2. R.A. Nordin, W. R., Holland, M. A. Shahid, "Advanced Optical Interconnection Technology in Switching Equipment", Journal of Lightwave Tech., Vol. 13, No. 6, June 1995.

3. David V. Plant, Andrew G. Kirk, "Very Short Reach (VSR) Optical Interconnects: Challenges and Solutions", McGill University, CITR Annual Meeting Presentation, Aylmer, Québec, August 27 - 28, 2001.

4. Christopher Tocci, John Caulfield, "*Optical Interconnection, Foundation and Applications*", Artech House, Boston USA; 1994.

5. H. Kkartensen, C. Hanke, "Parallel Optical Interconnection for Uncoded Data Transmission with 1 Gb/s-per-Channel Capacity, High Dynamic Range and Low Power Consumption", Journal of Lightwave Tech., Vol. 13, No. 6, June 1995.

6. B. Bostica, F. Delpiano, P. Pellegrino, L. Pesando, S. Ricchiuto, "Parallel 10-Channel Interconnect Receiver Module Operating over 4 Gbit/s Based on Silicon Optical Bench Technology", International Electron. Packaging Conference Proceedings, (InterPACK'99), Maui, Hawaii, USA, 13-19 July 1999.

7. R. Michalzik, K.J. Ebeling, et al., "High Performance VCSELs for Optical Data Links", IEICE Trans. Commun., Vol. E84-B, No. 5, May 2001.

8. A. Ohki, M. Usui, et al., "Development of 60 Gb/s-Class Parallel Optical Interconnection Module (ParaBIT-1)", IEEE Trans. Electron., Vol. E 84-C, No. 3, March 2001.

9. L. J. Norton, F. Carney, et al., "OPTOBUS™, A Parallel Interconnect Solution", IEEE Lasers and Electro-Optics Society 10th Annual Meeting (LEOS '97), Conference Proceedings, vol.2, Nov. 1997.

10. L.A. Buckman, K.S. Giboney, et al.,"Parallel Optical Interconnect", Lasers and Electro-Optics, CLEO 2000 Conference Proceedings, San Francisco, USA, May 2000.

11. A. Yuan, K. Giboney, et al., "Parallel Optical Interconnections Development at HP Labs", IEEE Lasers and Electro-Optics Society 10th Annual Meeting (LEOS '97), Conference Proceedings, vol.2, Nov. 1997.

12. V. Plickert, L. Melchior, et al., "Progress In Packaging of Parallel Optical Interconnects", IEEE Lasers and Electro-Optics Society 2000 13th Annual Meeting (LEOS 2000), Vol. 2, 2000.

13. Y.-M. Wong, D. Muehlner, et al., "Technology Development of a High-Density 32-Channel 16 Gb/s Optical Data Link for Optical Interconnection Applications for the Optoelectronic Technology Consortium", Journal of Lightwave Tech., Vol. 13, No. 6, June 1995.

14. Alvesta, "3100 Series Optical Tranceivers", Product Data Sheet, 2001. http://www.alvesta.com/products.html

15. Zarlink Semiconductors, "MFT62340 12-channel Transmitter - 2.5Gb/s per channel", Product Data Sheet, 2001. http://products.zarlink.com/partfinder/prodprofile.cgi?device=1007&path=products/product_finder/group:23

16. Picolight, "30 Gb/s Parallel Optical Interconnect", Product Data Sheet, 2001. http://www.picolight.com/products/30gbspoi.html

17. Agilent Technologies," 30 GBd Fiber-Optic Link for High-Volume, Short-Range Applications", Product Data Sheet, 2001. http://www.semiconductor.agilent.com/cgi-bin/morpheus/promotions/promotionsDetail.jsp?promoID=20163

18. The Optical Internetworking Forum (OIF), "Very Short Reach (VSR) OC-192/STM-64 Interface Based on Parallel Optics", Implementation Agreement, USA, December 2000. http://www.oiforum.com/

19. Nortel Networks, "10 Gb/s EA Modulator and laser with optional Etalon stabilization", Product Specification Sheet, USA 2001. http://www126.nortelnetworks.com/datasheets/pdf/ea10ew_21_10gbs_ea_mod_laser.pdf

20. JDS Uniphase, "54TR Series OC-48 Transponder with MUX/DEMUX (1310 and 1550 nm)", Product Specification Sheet, USA 2001. http://www.jdsu.com/Site/images/products/54TR.pdf

21. Blaze Networks, "Afterburner-XGSX, The 10 Gigabit CWDM Solution", Product Brief, USA, 2001. http://www.blazenp.com/pdf/10gbspec1.pdf

22. Xanoptix, "XTM-72, Next-Generation Optical Connections", Product Brochure, USA, 2001. http://www.xanoptix.com/xtm-72.pdf

23. TeraConnect, "Teraconnect Terminator Series™, High-Density Optical Transmit & Receive Modules", Product Data Sheet, USA, 2001. http://www.teraconnect.com/pdfs/t48series.pdf

24. A.V. Krishnamoorthy et al., "16X16 VCSEL Array Flip-Chip Bonded to CMOS VLSI Circuit", IEEE Photon. Tech. Lett., Vol. 12, No. 8, August 2000.

25. K. Droggemuller et al., "Current Progress of Advanced High Speed Parallel Optical Links for Computer Clusters and Switching Systems", Proceedings IEEE Electronic Components and Technology Conference, 2000.

26. F. Peters, D. Welch, M. Donhowe, G. Giaretta, P. Kolesar, "High Speed 850 nm VCSEL Transmission Over MultiMode Fiber", IEEE 802.3 Higher Speed Study Group, July 1999.

27. R. Michalzik et al., "40 Gb/s coarse WDM data transmission with 825 nm wavelength VCSEL's over 310 m of high-performance Multi-Mode Fiber", Proc. 26th Europ. Conf. On Opt. Comm., ECOC 2000, vol. 4, pp. 33-34, Munich, Germany, Sept. 2000.

28. L. B. Aronson, B. E. Lemoff, L.A. Buckman, D. W. Dolfi, "Low-Cost Multimode WDM for Local Area Networks Up to 10 Gb/s", IEEE Photo. Tech. Lett., Vol. 10, No. 10, Oct. 1998.

29. R.W. Herrick, S.F. Lim, H. Deng, Q. Deng, J.J. Dudley, M.R. Keever, T. Oh, M. Li, M. Tashima, L.A. Hodge, X. Zhang, J. Herniman, P. Evans, B. Liang, and C. Lei, "Highly reliable oxide VCSELs manufactured at HP / Agilent Technologies", Invited Paper, SPIE Conference.

30. B. Bostica, M. Burzio, F. Delpiano, P. Pellegrino, L. Pesando, " A Ten-Channel Optical Transmitter Module for Sub-System Interconnection Operating at λ= 1.3 μm up to 12.5 Gbit/s", IEEE Transactions on Advanced Packaging, Vol. 22, No. 3, August 1999.

31. M. Salzberg, "Testing and Characterization of a Parallel Optical Interconnect for a Scalable Routing System", Master's thesis, McGill University, 2001.

32. Agilent Technologies, "Agilent HFBR-712BP and HFBR-722BP Parallel Fiber Optic Modules – 850nm VCSEL Array Transmitter and Receiver 1 to 2.5 GBd per channel", Preliminary Data Sheet, USA, August 2001.

33. L.-G. Zei, S. Ebers, J. -R. Kropp, K. Petermann, "Noise Performance of Multimode VCSELs", IEEE Jour. Light. Tech., Vol. 19, No. 6, June 2001.

34. K. Petermann, "*Laser Diode Modulation and Noise*", Dorderecht, The Netherlands: Kluwer, 1991.

35. Nordx/CDT, "Optical Fiber Cable", Product Catalogue, Canada, 2000. http://prodshop.solutionxpert.com/cgi-bin/nordxcdt.storefront/634592860/Catalog/

36. Nordx/CDT, "Inter-channel Optical Crosstalk in 62.5um Parallel MMF fiber", Customer Service Representative, September 2001.

37. USConec, "MTP Connectors", Product Specification Sheet, USA, 2000. http://www.usconec.com/pages/product/connect/mtpcon/mainfrm.html

38. Agilent Technologies, "Agilent test board HFBR-7001 for HFBR-712BP Parallel Fiber Optic Modules – 850nm VCSEL Array Transmitter 1 to 2.5 GBd per channel", Preliminary Data Sheet, USA, August 2001.

39. Agilent Technologies, "Agilent test board HFBR-7002 for HFBR-722BP Parallel Fiber Optic Modules – 850nm PIN Array Receiver 1 to 2.5 GBd per channel", Preliminary Data Sheet, USA, August 2001.

40. Agilent Technologies, "HFBR-7001 Transmitter Test Board", Test Board Gerber File, USA, 2001.

41. Agilent Technologies, "HFBR-7002 Receiver Test Board", Test Board Gerber File, USA, 2001

Chapter 3 POI Crosstalk Definition and Mitigation Techniques

This chapter will define crosstalk in detail with special emphasis on optical crosstalk. It will also list interesting crosstalk mitigation techniques as found in the literature. It is important to note that the details of crosstalk mitigation techniques used by component vendors cannot be divulged due to the sensitive nature of such information.

3.1 Crosstalk Definition

POI crosstalk is divided into 3 main components: optical, electrical, and thermal [1]. We focus on optical and electrical crosstalk in this thesis. We do not consider thermal crosstalk in any detail and only provide a brief overview of thermal effects on POI performance for completeness.

3.1.1 Optical Crosstalk

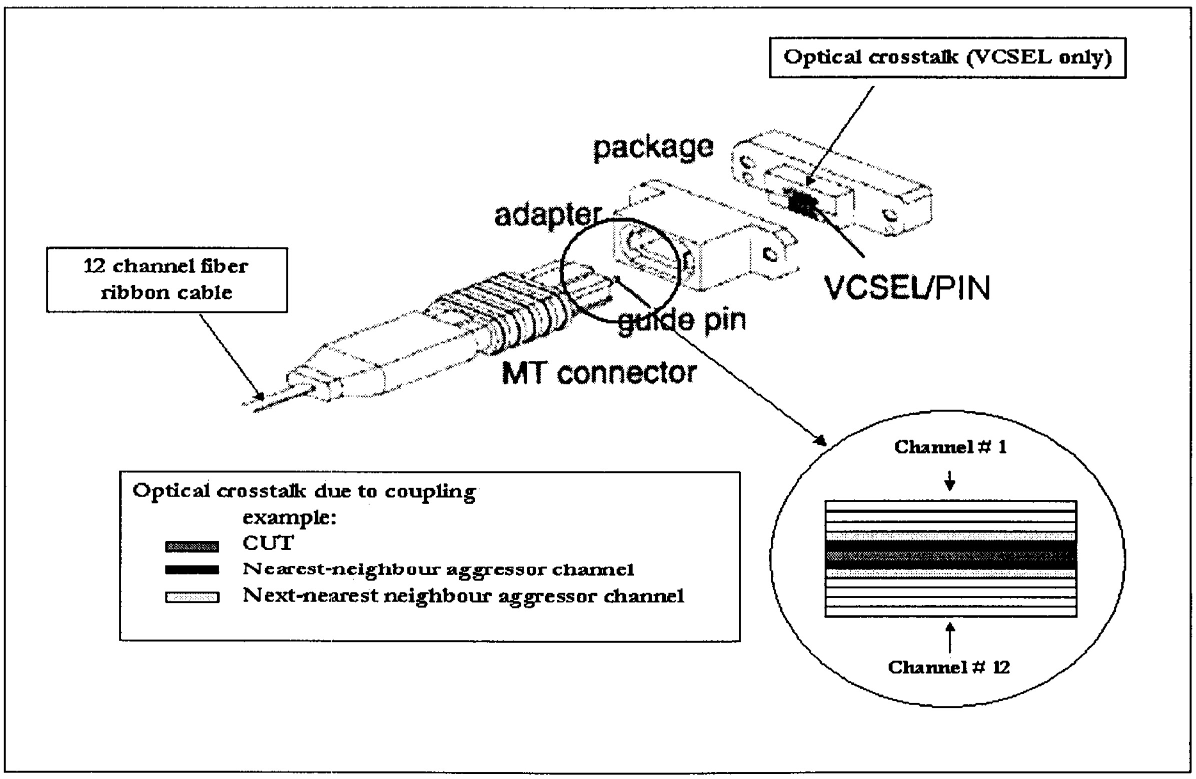

Figure 7: POI diagram with sources of optical crosstalk

From Figure 7, we define optical crosstalk, X, as

$$X = 10 \log \sum_{i=1}^{n} (P_{x-aggressors})_i / Pcut \quad \text{dB} \qquad \text{Equation (1)}$$

Where $P_{x\text{-aggressors}}$ is the optical power leaked from adjacent aggressor channels, P_{CUT} is the optical power of the channel under test (CUT) and "n" is the total number of neighboring channels (n = 11 in Figure 7).

Contributions to optical crosstalk in POI are threefold as can be seen from Figure 7:

1. Optical power leaks at the optical coupling sections (at the VCSEL and PIN arrays).

2. Spontaneous emissions from neighboring channels within the VCSEL array when VCSELs are very close to each other (less than 3 μm [2]),

3. Optical power leaks from channel to channel within the parallel optical fiber cable-here it is assumed to be zero as confirmed by suppliers (see Chapter 2).

3.1.1.1 Optical coupling at Tx and Rx

Optical crosstalk between POI channels can occur at both the transmitter and receiver ends, where the devices are coupled to the fiber medium [3]. Crosstalk will depend on the type of optical coupling used in the devices. If there is free-space between the active components and the fiber, then optical crosstalk is expected in systems using lens coupling. Butt coupling of the VCSEL/PIN arrays to the fiber will minimize crosstalk because it minimizes this air gap or free-space.

In the free-space case, it is also expected that optical crosstalk will be greater at the receive end than at the transmit end. Light typically needs to be tightly coupled into the fiber at the transmit end because of the large numerical aperture of the laser relative to the fiber. On the other hand, at the receive end, the coupling mechanism is often not as precise as at the transmit end and in some cases can even be lacking completely (free-space). Since photodiodes are also very sensitive, even a small incident optical crosstalk signal will generate unwanted photocurrent. The amount of optical crosstalk at the connector level will depend on the size of the air gap, which can vary depending on the connector insertion. Also note that as expected a larger active area of the photodiode will increase optical crosstalk since more of the incident optical crosstalk can be converted into an electric crosstalk signal [4].

Optical crosstalk due to coupling can be approximated by looking at the numerical apertures and pitch of the VCSELs, the active area and pitch of the photodetectors and the aperture of the fiber. A fine balance between all of these variables is needed to minimize crosstalk as will be shown in the example below. It is assumed that optical crosstalk will come mostly from the nearest neighbour and the next-nearest neighbour channels in a 1-D array VCSEL, i.e. at most 4 channels in a 1-D array [4]. However, in a 2-D array, optical crosstalk contributions could come from more than 4 neighbours depending on the location of the channel within the array [3].

As an example, we consider the POI described in chapter 2, with a pitch of 125 μm and a fiber numerical aperture (NA) of 0.2. We make the following assumptions:

- the optical signals obey Gaussian beam propagation properties with a beam waist, w(z), described in Equation 2 [29]:

    - $w(z)=w_o[1+(z+z_o)^2]^{1/2}$ Equation (2)

    where

        - z is the distance from the fiber end
        - w_o is the spot radius (at the fiber end)
        - $z_o= w_o^2(\pi/\lambda)$ (Raleigh number)
        - λ =845 nm

    - For small z, an additional components, $w^{\theta}(z)$ needs to be added to w(z) above:

- $$w^{\theta}(z)=z\tan^{-1}(\theta_{Gauss})$$ Equation (3)

  where

  - θ_{Gauss} = $\sin^{-1}$(NA)/1.5= 7.69 °=Gaussian divergence angle
  - $\sin^{-1}$(NA) = divergence angle containing 99% of optical power

- the surface areas of the photodetectors are all perfectly circular and equal
- the end of each one of the fibers within the POI cable lines-up perfectly with the center of the active area of the photodiode.

We can sum the results of equations 2 and 3 to get a rough approximation of the beam waist size at the detector area for different distances from the fiber. These are listed in Table 3 below.

Fiber Core Diameter	Beam waist at 12.5 μm from fiber (μm)	Beam waist at 25 μm from fiber (μm)	Beam waist at 50 μm from fiber (μm)	Beam waist at 100 μm from fiber (μm)
50 μm	26.69	28.38	31.76	38.53
62.5 μm	32.94	34.63	38.01	44.76

Table 3: Estimation of optical crosstalk due to optical coupling

The size of the beam diameter hitting the photodiode sensitive area grows slightly as the distance from the fiber end increases. However, it decreases with the diameter of the fiber core.

The amount of optical power that will hit an adjacent channel will be a function of the photodiode area radius and the pitch at which they are spaced from each other. Approximately 99% of the optical power will be confined in an area defined by a beam waist radius of 1.5 w(z). Hence a 50 μm detector size would detect 99% of the incoming optical power from the 50 μm fiber while a 60 μm detector would be needed with 62.5 μm fiber. Only a portion of the remaining 1% optical power could be detected by an adjacent photodetector. This 1% represents approximately 0.004 mW from the average optical transmit values obtained in Chapter 6, which is negligible.

Equation 3 below can be used as a quick check to verify if 99% of the energy is contained in 1.5 times the beam radius:

$$(PhotodiodeArrayPitch) - PhotodiodeRadius > SpotSizeRadius \qquad \text{Equation (4)}$$

If the conditions described in equation 4 are satisfied, there will be minimum optical crosstalk. It can be observed that a large photosensitive area combined with a small array pitch will increase the crosstalk contributions to adjacent channels. Since the mating design of the connector is such that the maximum air gap is less than 60 μm and the receiver sensitive area radius is less than 60 μm, optical crosstalk due to coupling inefficiencies is not foreseen in this experiment.

It is also interesting to note that decreasing the pitch to 62.5 μm would have significant impact on optical crosstalk. The photodiode radius would have to be reduced to a size smaller than of 31.25 μm. This photodetector size would not be optimum to receive at least 99% of the incoming optical power. Optical crosstalk would likely to occur in such conditions.

Optical crosstalk can be further subdivided into homodyne (same wavelength) and heterodyne (different wavelength) as well as coherent and incoherent [5]. Both types can influence the performance of a multi-link or multi-hop optical circuits used in O-MINs, as this will be explained later in Chapter 4. Since all POI channels run asynchronously and independently from each other in real life applications, we expect the crosstalk to be incoherent, i.e. the waveforms from adjacent VCSELs will be incoherent and data signals from adjacent channels will be uncorrelated.

3.1.1.2 Spontaneous emissions from neighboring channels

As described in [2], when VCSELs are very close to each other with less than 3 μm spacing, spontaneous emission of one VCSEL will change the apparent threshold of neighbouring channels through the creation of a significant number of photo-carriers. When a neighbouring channel is biased, its spontaneous emission reduces the threshold voltage of the channel under test. This effect is also reciprocal between the main channel and the adjacent channels. When both channels are biased, an increase in output optical power is expected.

3.1.2 Electrical Crosstalk

Electrical crosstalk contribution can be further subdivided into 2 main factors [3, 6]:

1. inductive and capacitive crosstalk between channels due to electrical conductors, similar to inductive coupling in the bond wires

2. current leakage between channels (due to the finite resistance between them)

3.1.2.1 Inductive and capacitance crosstalk between channels due to electrical conductors:

The predominant cause of electrical crosstalk in laser arrays is associated with ground loops and the parasitic inductance of the connections to the laser or photodiode [7]. Electrical crosstalk is frequency dependent. The dominant source of crosstalk is resistive coupling for low frequencies (< 700 MHz) [1 6, 8]. At higher frequencies, electromagnetic coupling becomes dominant. Figure 8 illustrates a 20 dB/decade increase in crosstalk as frequency increases and indicates that the dominant path of the crosstalk is an inductive coupling between channels [1], either induced by bond wires used to interconnect drivers to the lasers or by the inductive coupling through the ground contacts [8]. This makes sense since electromagnetic fields get stronger at high bit rates and couple between channels, especially "when rise/fall times are short and voltage swing is high" [9]. Electrical crosstalk in the experimental POI is therefore expected to be due mostly to inductive/capacitive coupling since the components will be operated at high frequencies, i.e. 2.5 Gb/s and higher during the experiments as well as real life applications. Similar behaviour is observed in photodiodes [26].

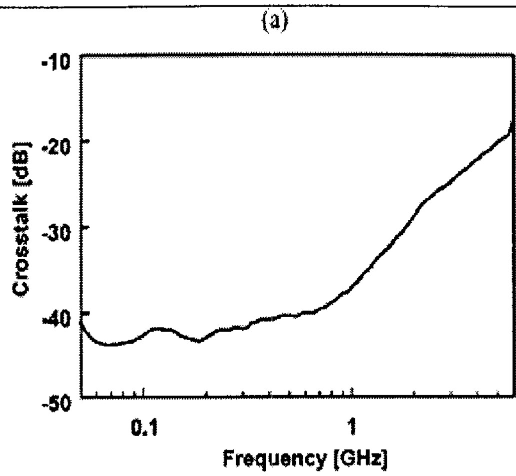

Figure 8: Graph of crosstalk versus device frequency [1]

Crosstalk can also vary between laser-pair within an array at high frequencies [8]. This variation depends on the laser position within the array.

Attention has to be paid also to the lengths of the wires between the VCSEL drivers and the lasers: different wire lengths will cause a difference in modulation characteristics of a multi-channel VCSEL because of the difference in channel impedance and capacitance [3]. As stated in Chapter 2, all VCSEL and PIN array wire lengths on the test boards used in this experiment were the same.

3.1.2.2 Current leakage between channels within the VCSEL/PIN

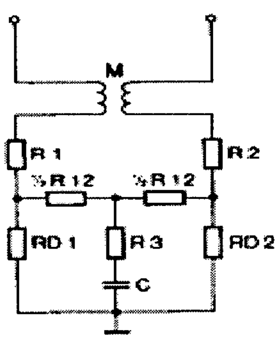

Figure 9: Electrical model of VCSEL array [6]

Inter-channel crosstalk between lasers in an array is due to the difference in resistance between the lasers at low frequencies. Figure 9 shows an electrical model of a VCSEL [6]. The cladding layer (R12), and the 2 laser diodes (RD1 and RD2) act as a current splitter: its splitting ratio depends on bias current, i.e. the small signal resistance of the laser diodes.

This difference in crosstalk is proportional to the physical distance between the 2 lasers (or photodiodes). The larger the spacing, the better the crosstalk suppression. For example, a 7dB difference in electrical crosstalk was observed between 2 channels when the physical spacing between the two lasers was varied from 100 μm to 500 μm [6].

Crosstalk also increases as the bias current of the neighbouring channels is decreased. This is illustrated in Figure 10 [1]. The larger the difference between bias currents of adjacent channels, the smaller the differential resistance of the neighbouring channels. This makes a larger part of the current injected into the adjacent channels flow into the VCSEL under test through electrical coupling [6]. However, under normal operation, all lasers of an array will be operating at the same bias current and this should not be a factor in the experiments done in this thesis.

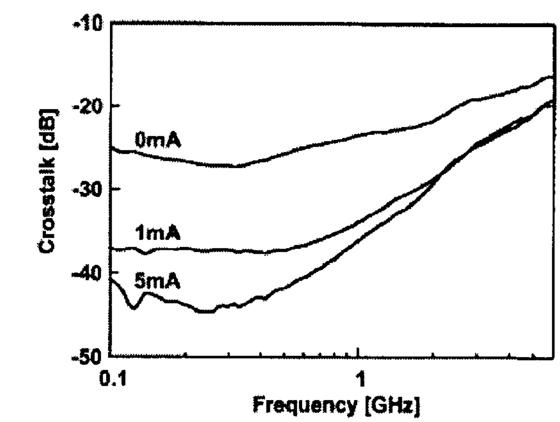

Figure 10: Graph of crosstalk versus frequency with different bias currents [1]

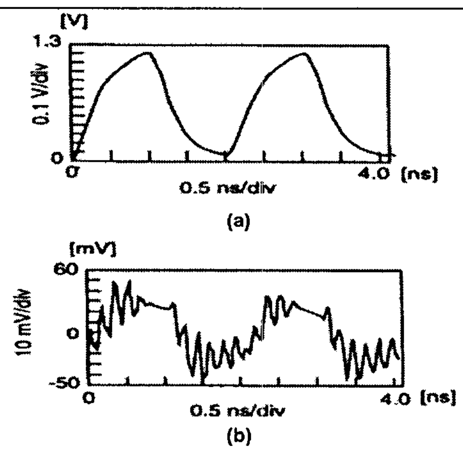

Figure 11: Results of a simulation to determine electrical crosstalk between the lines connecting a driver chip to a 32-channel VCSEL array [4]

Figure 11 shows results of a simulation done to measure the electrical crosstalk of the lines connecting the laser array driver chip to a 32 channel VCSEL array: Figure 11 b) illustrates that electrical crosstalk due to the two nearest neighbours represents about 4.5% of the active signal of 1.2V (shown in Figure 11 a)). This amount of crosstalk can be significant when very low system BER needs to be achieved [4].

3.1.3 Thermal Effects

As stated earlier, we will not experimentally characterize thermal crosstalk; for completeness, we list the sources of thermal crosstalk. The internal temperature compensating circuits of the POI components tested were proven to function properly as little variation in POI performance was observed at higher ambient temperatures [10]. Therefore, temperature changes will have little impact on crosstalk performance of the POI used in this thesis. It would be worthwhile, however, to inquire about the use of temperature compensating circuits before testing other POI component.

Thermal effects, if not properly compensated, represent an important aspect of the overall crosstalk performance of POI as they can affect channel performance and operating wavelength. Basically, temperature leaks from neighbouring channels into the main channel of a VCSEL array can cause enough of a temperature rise to decrease the output optical power of the main channel [11]. "As the main channel temperature increases, its gain decreases for a given injection current and its differential gain decreases due to both the temperature and increased carrier density required for threshold. With threshold current increasing and the differential gain decreasing the performance will degrade at higher temperatures" [12]. The thermal effects are even greater in 2-D VCSEL arrays and are shown to affect both light output power and emission wavelength [13].

Channel to channel thermal leaks or thermal crosstalk increases with the internal device temperature of the laser array. Temperature cycling or increased operating temperature has the additional negative effect of accelerated component aging. This highlights the importance of built-in temperature compensating mechanisms.

3.2 Crosstalk Mitigation Techniques

Because the exact structural details of the POI component studied in this thesis are either not available or are proprietary, this section will identify techniques used to minimize POI crosstalk that are found in literature, but not necessarily used in the components. These will be illustrated with examples where possible. The objective here is not to review the component structures in detail but rather to focus on the key attributes required by POI components to minimize crosstalk.

In general, 3 factors can be tailored to minimize crosstalk: the physical properties of the active components, the electrical/optical connection scheme, and the signalling schemes used to drive the components.

3.2.1 Optical Crosstalk Mitigation

Optical crosstalk can be minimized at the POI Tx and Rx modules and more specifically, at the active components of these modules, i.e. VCSEL and PIN arrays.

3.2.1.1 VCSEL based Tx Module

VCSEL structure

The 850 nm 12x2.5 Gb/s VCSEL arrays used in this thesis is based on oxide-confined technology [14], which provides better optical confinement properties than the older generation proton-implanted VCSEL arrays. Typically, this VCSEL structure consists of quantum wells sandwiched between top and bottom quarter wave DBR mirrors or Bragg reflectors with high reflectivity for feedback. The quantum wells are generally InGaAs/GaAs or AlGaAs/GaAs [15, 16]. The optical confinement provided by the oxide layers is strongly index-guided because of the large refractive index difference between the oxide and the active section. This improves coupling to the fiber as less diffraction occurs at the output of the VCSEL. The oxide layer also forms an aperture for the laser current and an optical waveguide at the same time [16]. A typical VCSEL structure is shown in Figure 12 [17] below.

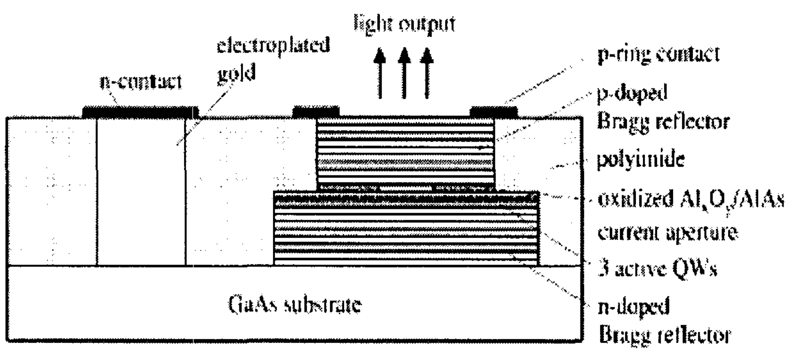

Figure 12: Example of a selectively oxidized top-emitting structure [17]

The improved optical confinement properties of oxide-confined VCSELs minimize inter-channel optical crosstalk.

Spontaneous emissions between channels can also be minimized through the device's structure. To block and isolate spontaneous channel emissions, absorptive and non-conductive films can be deposited on the VCSEL sidewalls, or walls can be added between the devices of the array [2]. Large spacing between the VCSELs should also minimize crosstalk due to spontaneous emissions.

Also a crosstalk reduction can be achieved by pre-biasing all devices slightly above threshold, typically at 1.1 times the threshold bias value. This will clamp spontaneous emissions. An example in [2] shows that when pre-biasing 2 channels at the same voltage, the total output power is very close to the sum of the individual operation powers of the 2 devices but the optical crosstalk is reduced to <-20 dB.

Coupling Mechanism:

Since light is transmitted and received normal to the VCSEL/PIN mounting plane, coupling light is typically normal, which means the light will require a turn before being coupled into the transmission fiber, like the 45 ° mirror shown in Figure 13.

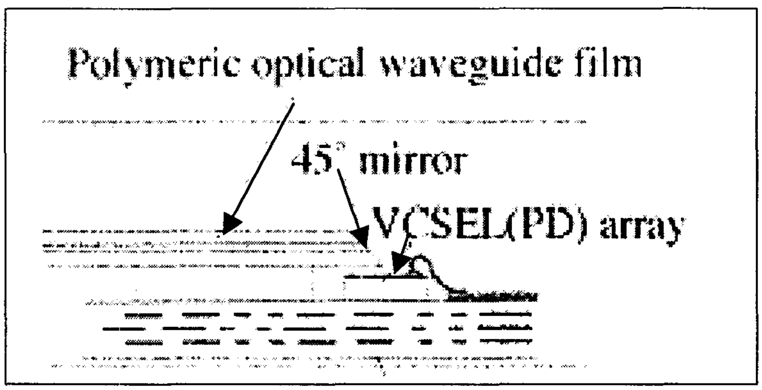

Figure 13: Coupling of VCSEL light emission in a fiber

No matter what scheme is used, the critical factor in the coupling of light from a VCSEL to a fiber or from a fiber onto the active area of the photodetector are the distance between the optoelectronics and the fiber medium and the lateral offset of the alignment. Sub-optimal distances and misalignment reduce the efficiency of the optical coupling, which result in optical power losses, leading to greater drive currents and power consumption [18]. In this thesis the component manufacturers are assumed to maintain very tight alignment tolerances.

Optical alignment tolerance will also affect the above parameters. A smaller core, lower NA fiber generally requires tighter alignment tolerances. Inefficient VCSEL light coupling causes larger drive current which leads to greater power consumption and radiated emissions. Of course, optical losses can affect crosstalk performance and reduce the system link budget.

Because the output aperture size of each VCSEL within an array can be lithographically controlled, their gain region can be made symmetrical to the output aperture, making their output profiles symmetric—this facilitates the packaging and the integration with fiber ribbons or micro-lenses for multi-channel POI.

Butt coupling is another very efficient coupling technique that can be used to couple light from a VCSEL in a fiber. Because the fiber is directly coupled to the VCSEL, it does not require a redirection mechanism. An optoelectronic array is butt-coupled to the MT connectorized optical ribbon fiber through an optical element, which manages the light from the optical arrays at Tx and Rx to the 62.5 μm MMF [14, 19].

Using index-matching material to fill air gap between the VCSELs and fibers can improve coupling between fiber and laser, but it is seldom used in practice.

If free-space coupling is required, reflective mirrors with low polarization sensitivity are needed on the reflecting mirrors in order to keep polarization fluctuations from being converted to amplitude noise on the fiber ends. Gold is typically the best metal for mirror coating. An interesting approach is shown in [4]: 62.5 μm core GRIN MMF is coupled to VCSEL/PIN arrays via 45 degree mirrors polished onto the ends of the fibers. Again this is impractical for real-life applications.

3.2.1.2 PIN based Rx Module

On the Rx side, the diameter of the photodiode determines the Rx bandwidth and alignment tolerances [16]. The size of the active area of the photodiodes within a PIN array will affect the crosstalk performance of the Rx module. For standard 62.5 μm graded-index fiber into the photodiode, a diameter considerably larger than the core is required for lens-free coupling. The GaAs PIN photodetectors used in this experiment have a diameter smaller than 87.5 μm [1, 14, 19]. Likewise, another supplier also uses a large active area of 95 μm for its InGaAs/InP PIN photodiodes arrays [16].

3.2.1.3 MMF Fiber Ribbon

Smaller core MMF, i.e. 50 μm core MMF fiber instead of the standard 62.5 μm core MMF will relax the coupling tolerances at the receive end of a POI but will tighten them at the transmit end.

3.2.1.4 Notes on Optical Crosstalk Suppression in O-MIN architectures:

Optical crosstalk can be further suppressed at the optical redirection box with the use of MUX/DEMUX and optical filters at the optical inputs. Also note that wavelength deviations with temperature changes must also be kept to a minimum since optical MUX/DEMUX are tuned to specific wavelengths.

3.2.2 Electrical Crosstalk Mitigation

Electrical crosstalk can be minimized at the Tx and Rx modules of the POI and more specifically, at the active components of these modules, i.e. VCSEL and PIN arrays.

3.2.2.1 VCSEL based Tx Module:

Structure

Oxide confined VCSEL arrays with deep trenches, very short driver lines of same length, and differential signalling scheme will minimize crosstalk at the transmit module.

Oxide-confined VCSELs also provide better carrier confinement than proton-implanted VCSELs and can offer low threshold current, high overall efficiency, and freedom from any bias control [1]. Since the oxide layers are located immediately adjacent to the active region, they insulate and confine the charge carriers into the quantum wells. This provides better carrier confinement, which not only reduces electrical crosstalk but also reduces threshold current and minimizes threshold deviation across the array. Threshold currents as low as 100 μA have been demonstrated [20, 21]. Also threshold currents deviations as low as 50 μA, and even 14 μA across arrays have been shown [16, 21]. Minimum threshold current deviation leads to improved array performance: a small threshold current deviation is an indication that current leakage across VCSELs in the array is low and electrical crosstalk is thus minimized.

Of course, electrical crosstalk can be reduced by isolating the channels within an array through isolation trenches or semi-insulating substrates and deep trenches etched through the n-DBRs [16]. This prevents inter-channel coupling through the common n-layer.

Connection Scheme

The electrical connection scheme will also influence crosstalk performance of the active modules. Short signal lines will help minimize crosstalk. Signal lines terminated very close to the driver chip on the Tx module minimize electrical crosstalk [4]. On the components used in this thesis, high-speed digital signals are routed on a flex circuit from the BGA onto the Tx or Rx ICs of the Rx module [14, 19]. Also, a Silicon based bipolar transmitter/receiver IC is mounted as close as possible to the optoelectronic components for enabling high-speed operation [14, 19].

Inserting ground wires or power leads between signal leads or shielding each individual line will isolate signal leads from one another and reduce electrical crosstalk [3, 15]. Using electrical fan-in/out microstrips on ceramic with matched impedance has been shown to minimize electrical crosstalk [23] especially if they are shielded [24]. A π filter, which filters out the noise due to the current switching of the laser drivers of the array, can also be used at the input of each current source [23].

Signaling Scheme

The scheme used to drive the Tx module impacts the crosstalk performance of these components. Differential input voltages are used to drive laser and Rx modules used in this experiment [25]. Because power and ground currents tend to cancel in the differential links, crosstalk is reduced [18]. Differential signalling provides the additional benefit of lower power consumption: using a differential signalling scheme cuts power consumption in half compared to single ended connections having the same nominal SNR. For example, LVDS signalling can further reduce total power consumption and guarantees compatibility for large number of datacomm IC's [16].

3.2.2.2 PIN based Rx Module

Physical Properties

GaAs-based photodiode arrays suffer from electrical crosstalk issues similar to those found in VCSEL array based Tx modules. These can be minimized using several different techniques: increasing the spacing between conductors; using wide and deep notches in the substrate to separate the channels, and shielding the conductors. Shielding can be integrated monolithically, as was done in [26] for a 1.55 μm PIN array. Like with the Tx module, high sensitivity, minimum current leakages and maximum electrical output uniformity are also desired across the Rx array. This can be achieved as shown in [15], where an Rx sensitivity of 0.4 mA/mW and leakage currents (2V bias voltage) of 40 nA for a 60 μm diode and 50 nA for a 70 μm diode were reported. The overall uniformity of this component was better than 1 dB with mean output currents of 200 μA and a max deviation of ± 32 μA.

Connection scheme:

The schemes described for the VCSEL-based Tx module also apply to the Rx module.

Signaling Scheme

As for the Tx module, a differential signalling scheme will minimize crosstalk at the Rx array as well. In addition, it is also important to control the amplitude of the integrated amplifier array: an output stage providing full ECL swing, and amplitude control will lower jitter and crosstalk at maximum operation speed [15].

3.2.3 Notes on temperature compensating techniques

As shown with the components used in this experiment [10], temperature compensation techniques can maintain the optical output power constant despite fluctuations in internal device or channel temperature. The temperature compensating method can be either structural or depend on external feedback monitoring.

At the structural level, the offset-gain method can be used to improve the VCSEL performance with temperature changes. Basically the wavelength of the cavity is longer than the peak gain (red-shifting) so that both converge during ambient temperature rise [4, 27]. This also minimizes channel-to-channel wavelength variation due to temperature changes.

Isolating channels thermally from one another minimizes thermal leaks from channel to channel. Evidently, thermal isolation between channels of an array increases with laser spacing. The thermal resistance determines the internal device temperature: lasers in the center of an array exhibit a higher thermal resistance since more devices surround them. The temperature at the center of an array is typically the highest: it was shown to be 50 % higher at center then on the edges of the 2-D array [13].

Additional control inputs can maintain uniform laser power levels in the presence of temperature and supply voltage variations as well as device aging. Feedback from a monitor laser and detector is needed though. The monitor detects any temperature or supply voltage changes. It raises the bias and modulation currents of laser drivers accordingly in order to maintain uniform modulation currents. Therefore, at higher temperatures the laser current increases for a fixed voltage thus compensating for the lower optical gain. The output power stays almost constant for the entire temperature range [28]. However such circuits increase component cost, which represents an issue for multi-stage router applications as described in Chapter 1.

3.3 Summary

POI crosstalk is composed of optical, electrical and thermal components. Optical and electrical crosstalk is detailed in this chapter. The key attributes for minimizing POI crosstalk within the context of the VCSEL/PIN array components considered in this thesis are:

1. Oxide-confined MQW VCSELs

2. PIN photodiodes

3. Minimum optical coupling distance

4. Very short traces between active components and driver components

5. Shielded signal traces

6. Differential signaling scheme

7. Temperature compensating structure and/or circuits

This list of attributes can serve as a guideline when evaluating optical components to be used in high-bandwidth interconnects for scalable router applications. The same attributes can apply to next-generation 2-D array devices as well.

3.4 References

1. S. Nakagawa, S. -Y. Hu, D. Louderback, L. A. Coldren, "RF Crosstalk in Multi-Wavelength Vertical-Cavity Surface-Emitting Laser Arrays", IEEE Photon. Tech. Lett., Vol. 12, No. 6, June 2000.

2. S.-Y. Hu, J. Ko, O. Sjolund, L.A. Coldren, "Optical Crosstalk in monolithically integrated multiple-wavelength VCSEL arrays for multimode WDM local-area networks", Electron. Lett., Vol. 34, No. 7, April 1998.

3. Nam-Hyong Kim, "2-D Free-Space Optical Backplane Using Vertical Cavity Surface Emitting Laser", Master's Thesis, Department of Electrical Engineering, McGill University, Montreal, Canada, July 1996.

4. Y.-M. Wong, D. Muehlner et al., "Technology Development of a High-Density 32-Channel 16 Gb/s Optical Data Link for Optical Interconnection Applications for the Optoelectronic Technology Consortium", Journal of Lightwave Tech., Vol. 13, No. 6, June 1995.

5. P.J. Legg, D.K. Hunter, et al., "Inter-Channel Crosstalk Phenomena in Optical Time Division Multiplexed Switching Networks", IEEE Photon. Tech. Lett., Vo. 6, No. 5, May 1994.

6. G. Heise, "Crosstalk Investigation of Laser-Diode Pairs", IEEE Photon. Tech. Letters, Vol. 2, No. 2, Feb. 1990.

7. T. C. Banwell, A.C. Von Lehmen, R.R. Cordell, "VCSE laser Transmitters for Parallel Data Links", IEEE Journal of Quantum Elec., Vol. 29, No. 2, Feb. 1993.

8. M.W. Maeda et al., "Multigigabit/sec Operation of 16-Wavelength Vertical Cavity Surface Emitting Laser Array", IEEE Photon. Tech. Lett., Vol. 3, No. 10, Oct. 1991.]

9. S. Toupin, "Further Questions from Hyperchip", e-mail communication, Agilent Technologies, November 2001.

10. M. Salzberg, "Testing and Characterization of a Parallel Optical Interconnect for a Scalable Routing System" Master's thesis, McGill University, 2001.

11. M. Kajita, et al., " Temperature Characteristics of a Vertical-Cavity Surface –Emitting Laser with a Broad-Gain Bandwidth", IEEE Journal of Select. Topics in Quantum. Electron., Vol. 1, No. 2, June 1995.

12. F.H. Peters and M.H. MacDougal, "High-Speed High-Temperature Operation of Vertical Cavity Surface Emitting Lasers", IEEE Photon. Tech. Lett., Vol. 13, No. 7, July 2001.

13. T. Wipiejewski, D.B. Young, B.J. Thibeault, L.A. Coldren, "Thermal Crosstalk in a 4X4 Vertical-Cavity Surface-Emitting Laser Arrays", IEEE Photon. Tech. Lett., Vol. 8, No. 8, Aug. 1996.

14. L.A. Buckman, K.S. Giboney, et al.,"Parallel Optical Interconnect", Lasers and Electro-Optics, CLEO 2000 Conference Proceedings, San Francisco, USA, May 2000.

15. H. Kkartensen, C. Hanke, et al., "Parallel Optical Interconnection for Uncoded data Transmission with 1 Gb/s-per-Channel Capacity, High Dynamic Range and Low Power Consumption", Journal of Lightwave Tech., Vol. 13, No. 6, June 1995.

16. K. Droggemuller, et al., "Current Progress of Advanced High Speed Parallel Optical Links for Computer Clusters and Switching Systems", Proceedings IEEE Electronic Components and Technology Conference, 2000.

17. D. Wiedenmann, R. King, C. Jung, et al., "Design and Analysis of Single-Mode Oxidized VCSEL's for High Speed Optical Interconnects", IEEE Journal of Selected Topics in Quantum Elec., Vol. 5, No. 3, May/June 1999.

18. C. Wilmsen, H. Temkin, L.A. Coldren "*Vertical-Cavity Surface-Emitting Lasers, Design, Fabrication, Characterization and Applications*", Cambridge University Press, 1999.

19. A. Yuan, K. Giboney, et al., "Parallel Optical Interconnections Development at HP Labs", IEEE Lasers and Electro-Optics Society 10th Annual Meeting (LEOS '97), Conference Proceedings, vol.2, Nov. 1997.

20. L. A. Bergman, C. Yeh, J. Morookian, "Advances in Multi-Channel Optical Multi-Gbytes/sec. Bit-Parallel WDM Single Fiber Link", 50th Electronic Components and Technology Conference 2000, Conference Proceedings, 2000.

21. R. Michalzik, K.J. Ebeling, et al., "High Performance VCSELs for Optical Data Links", IEICE Trans. Commun., Vol. E84-B, No. 5, May 2001.

22. L. B. Aronson, B. E. Lemoff, L.A. Buckman, D. W. Dolfi, "Low-Cost Multimode WDM for Local Area Networks Up to 10 Gb/s", IEEE Photo. Tech. Lett., Vol. 10, No. 10, Oct. 1998.

23. B. Bostica, M. Burzio, F. Delpiano, P. Pellegrino, L. Pesando, " A Ten-Channel Optical Transmitter Module for Sub-System Interconnection Operating at $\lambda = 1.3\ \mu m$ up to 12.5 Gbit/s", IEEE Transactions on Advanced Packaging, Vol. 22, No. 3, August 1999.

24. B. Bostica, F. Delpiano, P. Pellegrino, L. Pesando, S. Ricchiuto, "Parallel 10-Channel Optical Interconnect Receiver Module Operating over 4 Gb/s Based on Silicon Optical Bench Technology", Proceedings International Electronic Packaging Conference 9InterPACK 99), Maui, Hawaii, USA, July 1999.

25. Agilent Technologies, "Agilent HFBR-712BP and HFBR-722BP Parallel Fiber Optic Modules – 850nm VCSEL Array Transmitter and Receiver 1 to 2.5 GBd per channel", Preliminary Data Sheet, USA, August 2001.

26. K.C. Syao, K. Yang, X. Zhang, et al., "Investigation of Adjacent Channel Crosstalk in Multichannel Monolithically Integrated 1.55 μm Photoreceiver Array", Journal of Light. Tech., Vol. 15, No. 10, October 1997.

27. R. Michalzik, R. King, F. Mederer, M. Kicherer, G. Giaretta, K. Ebeling, "Short-Wavelength Vertical Cavity Surface Emitting Laser Applications: from High-Throughput Multimode Fiber Links to Two-Dimensional Interchip Interconnections", Soc. Of Photo-Opt. Instrumentation Eng., Opt. -Eng. 40(7), pp. 1179-1185, July 2001.

28. H. Kosaka, A.K. Dutta, K. Kurihara, Y. Sugimoto, K. Kasahara, "Gigabit-Rate Optical-Signal Transmission Using Vertical-Cavity Surface-Emitting Lasers with Large-Core Plastic-Cladding Fibers", IEEE Photon. Tech. Lett., Vol. 7, No.8, Aug. 1995.

29. B.E.A. Saleh, M.C. Teich, "*Fundamentals of Photonics*", John Wiley and Sons Inc., USA, 1991.

Chapter 4 Impact of Crosstalk on POI and System Performance

This chapter will explain how crosstalk not only affects the performance of a POI link but will also provide an overview of its impact on the scalability of systems based on O-MIN architectures.

4.1 *Impact of Crosstalk on POI performance*

4.1.1 Total crosstalk

Total crosstalk, i.e. the combination of optical, electrical, and thermal crosstalk, will dictate general POI performance. In the system applications considered in this thesis, all channels are driven simultaneously. The data integrity of a single POI channel is reduced by the total cross-talk contributions of the other channels within the same POI. The combination of electrical, optical, and thermal crosstalk degrades the link BER and consequently limits the optical link budget. This performance reduction is typically characterized by a power penalty due to a reduction in extinction ratio and increased jitter sensitivity. "The crosstalk measured through the optical signal includes all the possible crosstalk sources, and this data is the most meaningful"[1]. When measuring crosstalk, power and jitter penalties can be determined [2]. Determining these penalties will lead to a more realistic view of the system performance as will be shown in Chapter 5 and Chapter 6.

The impact of crosstalk on link budget, jitter tolerance and performance uniformity across the array will be studied in this thesis. These parameters are detailed for single channels in [3] but will be expanded in Chapter 5 and Chapter 6 to include multi-channel operation and to determine the different crosstalk components.

Accurate link budgeting depends on worst-case analysis of the power penalty and jitter penalty due to POI crosstalk. For shelf-to-shelf interconnect applications used in O-MINs, it is important that each POI channel offer the same performance attributes in order to ensure overall system stability. Optical crosstalk can further limit system scalability in O-MIN architectures using redirection boxes as will be seen in the next section of this chapter. As stated earlier, we will not consider the impact of temperature variations on POI performance in this thesis.

Typically inter-channel skew is also considered a performance parameter. In the application studied in this thesis, individual POI channels are considered independent from each other and thus inter-channel skew is not a factor.

4.1.2 Power Penalty Due to Crosstalk

The power penalty associated with component crosstalk is observed by comparing the BER versus Rx Sensitivity curves of a single channel operating with that of the same channel operating simultaneously with all the other channels in the array. These curves were explained in detail in [3] and are typically used to evaluate the performance of a POI link. A 1 dB power penalty is observed when all 1.25 Gb/s channels are turned on (10^{-12} BER) as shown in Figure 14 [2]. The power penalty observed when operating all the channels in the device at the same time is attributed to inter-channel (optical and electrical) crosstalk at both transmit and receive ends of the POI. It will be interesting to identify the main cause of this power penalty, as it needs to be evaluated accurately for real-life link budgets.

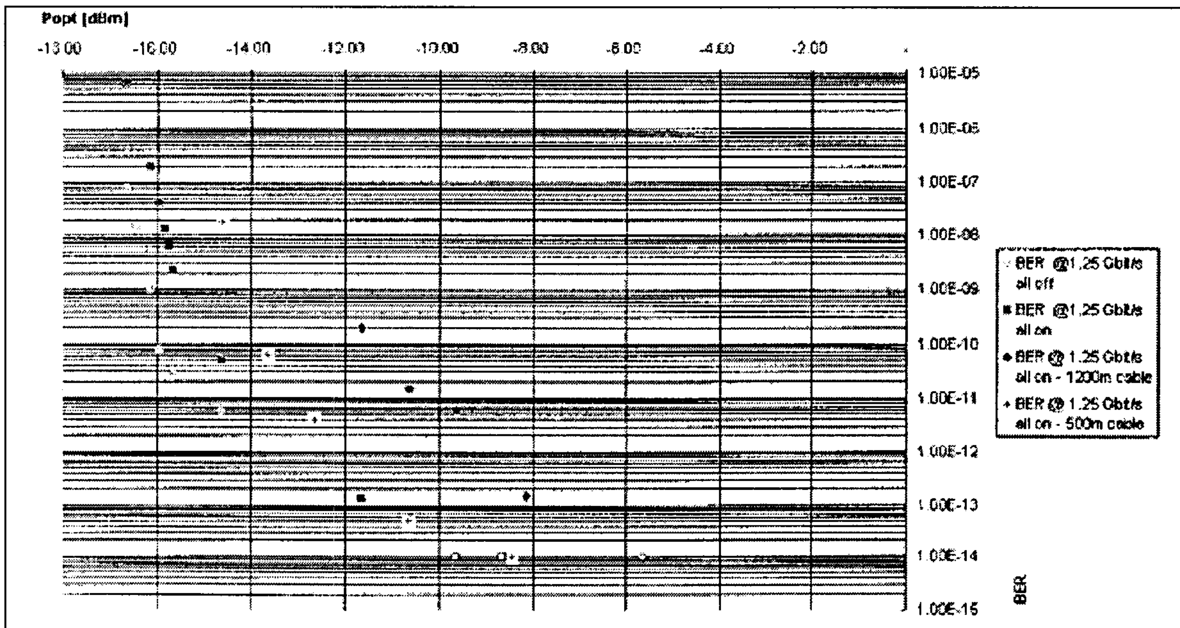

Figure 14: Example of a waterfall curve showing a power penalty due to crosstalk [2]

The power penalty due to POI crosstalk is expected to be non-uniform across channels: a smaller penalty is expected for the side channels of the array as they have fewer neighbors that can potentially contribute crosstalk signals. Thus, one of the objectives in crosstalk evaluation is to determine the channel with the worst power penalty within the array since this channel will ultimately define the system link budget. The worst case channel(s) is expected to be the one(s) with the most neighbors, i.e. the middle channels within a 1-D and 2-D array, but this will be dependent on the physical structure of the VCSEL and photodiode arrays.

4.1.3 Jitter Tolerance

Jitter performance of the POI has been analyzed in detail using a "bathtub curve" generated with the sampling point method [3] (this is basically a BER versus eye position curve). An example is shown in Figure 15 [3]: 25% degradation in jitter performance (Figure 15 b) over single channel operation (Figure 15 a) is observed when operating all channels simultaneously for an Rx sensitivity of –12 dBm and a 10^{-12} BER. The effects of jitter on link performance are especially important for high-speed links, as they will also translate into a power penalty [4]. A degradation of single channel jitter performance is expected as multiple channels are operated simultaneously. Deterministic Jitter (DJ) influences the eye opening thus changing the starting points of the bathtub walls resulting in a closure in eye opening. Random Jitter (RJ) affects the slope of the bathtub curve. We will focus on the impact of inter-channel crosstalk (optical and electrical) on the jitter performance of the POI link and more specifically, on total jitter [3, 5]. Again, the jitter penalty due to multi-channel operation needs to be evaluated accurately to determine the link budgets of POI links used in O-MIN applications. Tolerance to jitter variations will lead to improved system stability.

A stated in Chapter 1, a 10^{-14} BER performance is typically required from POIs to provide carrier-class system reliability. However, the specifications of the serial-to-parallel electrical signal converters used in conjunction with the POI only allow for a 10^{-12} BER. This is sufficient in the present application following [3, 6]. Therefore the total jitter budget for the POI link is 120 ps for the Tx, 20 ps for the fiber link and 95 ps for the Rx for a total POI budget of 177 ps or 0.59 UI (Unit Interval) with a 10-20% jitter performance degradation when all POI channels are operating simultaneously (4 meters of fiber) [6]. For comparison purposes a total jitter in the eye crossing of 83 ps was observed in [7] when driving 12 channels of a VCSEL array at 2.5 Gb/s with a PRBS 2^{15}-1. This shows that it is possible to meet the system jitter budget with commercially available components (but the actual POI performance will be measured in the next chapters).

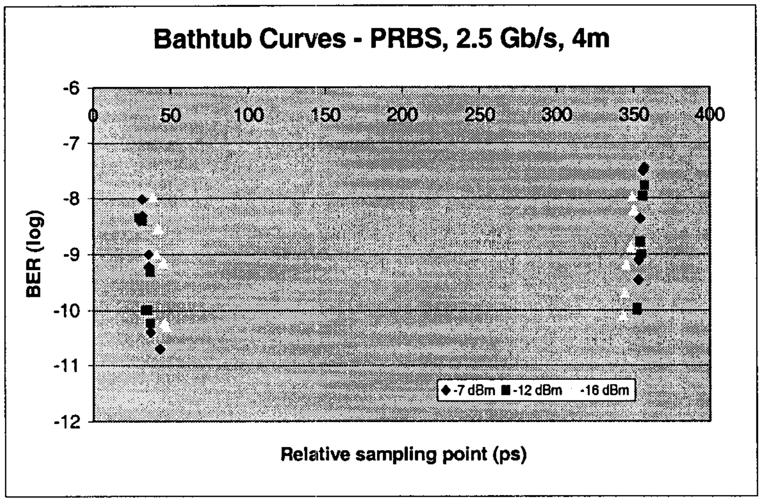

a) Single-channel bathtub curves for channel 9 at 2.5 Gb/s, 4 meters

2.5 Gbps	Eye opening	
BER(log)	**-7 dBm**	**-12 dBm**
-5	85.0%	85.7%
-6	83.7%	84.3%
-7	82.3%	83.0%
-8	80.9%	81.7%
-9	79.6%	80.3%
-10	78.2%	79.0%
-11	76.8%	77.6%
-12	**75.5%**	**76.3%**
-13	74.1%	74.9%
-14	72.7%	73.6%
-15	71.4%	72.2%

Table 4: Single-channel bathtub curve for 4m., 2.5 Gb/s

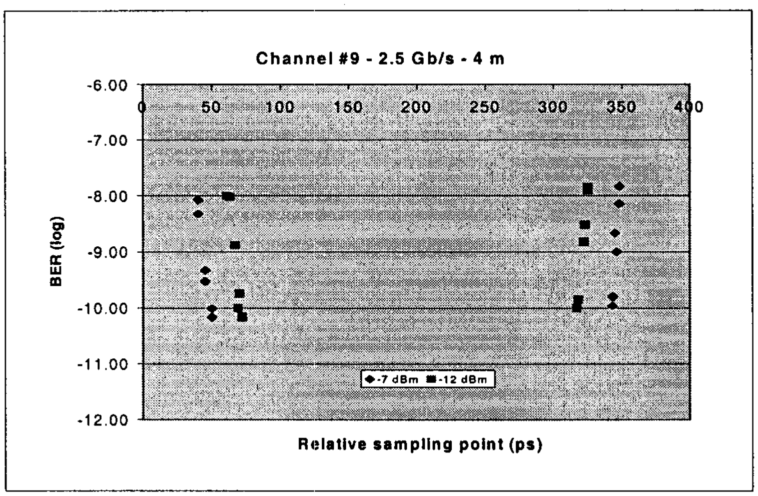

b) Multi-channel bathtub curve for channel 9 at 2.5 Gb/s, 4 meters

2.5 Gbps	Eye opening	
BER(log)	**-7 dBm**	**-12 dBm**
-5	83.5%	72.0%
-6	81.5%	69.9%
-7	79.4%	67.8%
-8	77.4%	65.7%
-9	75.4%	63.6%
-10	73.3%	61.5%
-11	71.3%	59.4%
-12	**69.3%**	**57.3%**
-13	67.3%	55.3%
-14	65.2%	53.2%
-15	63.2%	51.1%

Table 5: Multi-channel bathtub curve for 4m., 2.5 Gb/s

Figure 15: Example of a bathtub curve showing a jitter penalty due to crosstalk [3]

4.1.3.1 Bit-rate induced power penalty

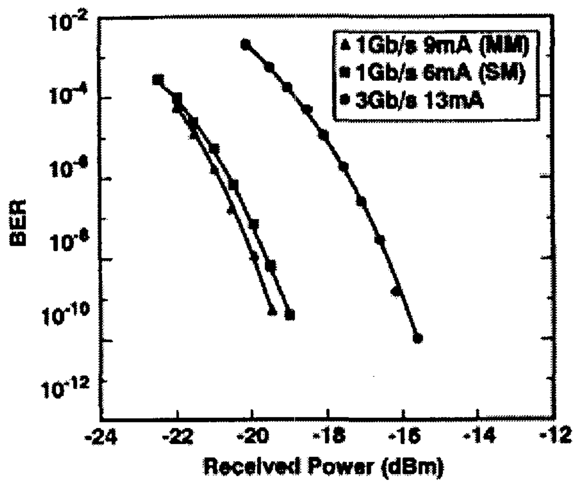

Figure 16: Graph showing a received power penalty when the bit rate increases (for MMF and a given BER)

Increasing bit rate across the POI array will impose an additional power penalty [4, 8, 9]. Figure 16 shows a power penalty of approximately 3.5 dB for a 10^{-12} BER as the bit rate is increased from 1 Gb/s to 3 Gb/s [10]. This penalty is due to the fact that receiver-switching power depends on bit rate [4]. Also note that dispersion is not a factor in this case.

The impact of bit rate on the crosstalk performance of the POI will be analyzed in this thesis since it is planned to increase the POI bit rate during the lifetime of the O-MIN system. Therefore this penalty will need to be considered when establishing the fiber link budget of the O-MIN as it is preferable to not modify the system link budget once the system fiber links of an O-MIN are installed.

4.1.4 Uniformity

As stated in Chapter 2, if the performance is uniform across the array, complicated control circuitry is not required, thereby keeping the components inexpensive.

The uniformity of the optical crosstalk across the array needs to be evaluated. This will be important in a POI application with redirection boxes since optical circuit lengths can vary within the system as shown in Figure 4. Uniformity across POIs enables uniform link budgets across all the optical channels of an O-MIN architecture.

Good performance uniformity is characterized by sensitivity deviations below +/- 1 dB for all channels at all the data rates for which the devices are designed to operate [7]. Also note that threshold current uniformity is needed to ensure uniform control of the optoelectronic arrays [10].

4.2 Impact of Crosstalk on O-MIN Performance

Optical multi-stage networks (O-MIN) described briefly in Chapter 1 show great promise for scalable router architectures. However, crosstalk challenges need to be better understood to enable the scaling of these systems using optical interconnects. In addition to the power penalty due the crosstalk within the POI itself, the crosstalk suppression properties of the optical redirection box can further limit O-MIN scalability. Understanding and minimizing the impact of these crosstalk penalties is a unique challenge. A general overview will be presented in this section and is subject to further research.

Optical crosstalk within the redirection box (RB) can represent such a problem that different MIN architectures have been proposed to avoid or minimize this particular problem [11, 12, 13, 14,15]. " Switch (RB) crosstalk is the most significant factor which reduces SNR and limits the network size" [15]. This is validated by a number of studies that evaluate the impact of RB crosstalk on system performance [16-26]. However, by attempting to solve the crosstalk issues associated with the redirection boxes, some of the proposed architectures actually create further system limitations. For example, [12] solves the crosstalk issue by using switch dilation to reduce crosstalk at the RB but dilation actually increases the insertion loss penalty at the RB, thereby reducing the overall permissible optical power penalty between MIN nodes and subsequently the configuration flexibility. Using semiconductor optical amplifiers (SOA) or other optical amplification schemes does overcome the insertion loss problem but it creates SNR challenges since ASE noise accumulates as the network scales. This degrades the performance of the O-MIN as suggested in [16]. Also numerous optical components required to create the O-MIN suggested in [16] will increase the cost. Other proposed solutions presented are rather complex in terms of RB equipment or algorithms needed for their management, and are expensive—this is contrary to the low system cost requirement expressed in Chapter 1.

We are not aware of any studies describing the impact of POI crosstalk on O-MIN scalability. However a number of studies exist detailing the scalability of all-optical networks using optical redirection boxes (optical cross-connects) and SMF fiber (basically used in optical backbone architectures) [16 to 26]. It is thus interesting to try to draw a parallel between these two, as the basic principles described are the same.

Component crosstalk has been shown to limit the scalability of all-optical networks using optical cross-connects as redirection boxes [17-21, 23-26]. In summary, crosstalk suppression of greater than –40 dB is required between RB channels for SMF all-optical networks using RBs, [16, 25, 26]. This crosstalk suppression requirement becomes even more stringent at higher bit rates [25].

However, in the case of an O-MIN, the optical signals coming into an optical redirection box from a POI might already have an optical crosstalk component. This crosstalk, especially if caused by the Tx, can add to the crosstalk already inherent to the RBs and degrade further the performance of the optical link between 2 shelves linked with POIs. In addition, the optical crosstalk component found at the receive end of a POI link will also degrade the link performance and system scalability further. As the O-MIN scales through interconnection of many RBs, the scalability of the O-MIN will degraded with the POI link BER. Thus, crosstalk within POI technologies can potentially limit the scalability of O-MIN networks, since signals coming into the RB will have already been degraded by the inherent optical crosstalk associated with POI. As stated earlier, crosstalk suppression of greater than –40 dB is expected for RBs used in all-optical networks. Similar stringent crosstalk requirements will be expected on RBs used in scalable router architecture. This will need to be evaluated in greater details in another study.

The optical crosstalk of the POI at the RB can be further characterized as homodyne crosstalk since, in general, the VCSEL wavelengths within an array are centred on the same wavelength. However, if CWDM technology is used within an array to minimize the fiber count in a link, then heterodyne crosstalk at the RB will also affect the scalability of the system. In the application described in this thesis, since all channels of the VCSEL/PIN array are operated independently, it is assumed that the crosstalk would also be incoherent at the RB. This would also need to be verified.

4.3 Summary

The impact of crosstalk on the key POI performance parameters was reviewed in this chapter. Of importance for optical interconnect applications are BER, jitter and performance uniformity across the POI channels. The impact of POI crosstalk on the performance of an O-MIN has also been discussed in this chapter. This information will serve as the basis for understanding the issues that will be presented in the next chapters.

4.4 References

1. S. Nakagawa, S. -Y. Hu, D. Louderback, L. A. Coldren, "RF Crosstalk in Multi-Wavelength Vertical-Cavity Surface-Emitting Laser Arrays", IEEE Photon. Tech. Lett., Vol. 12, No. 6, June 2000.

2. B. Bostica, M. Burzio, F. Delpiano, P. Pellegrino, L. Pesando, " A Ten-Channel Optical Transmitter Module for Sub-System Interconnection Operating at λ= 1.3 μm up to 12.5 Gbit/s", IEEE Transactions on Advanced Packaging, Vol. 22, No. 3, August 1999.

3. M. Salzberg, "Testing and Characterization of a Parallel Optical Interconnect for a Scalable Routing System", Master's thesis, McGill University, 2001.

4. A Z. Shang, A.P. Tooley, "Digital Optical Interconnects for Networks and Computing Systems", Journal of Lightwave Tech., Vol. 18, No. 12, Dec. 2000.

5. N. Schmitt, and D. Grant, "Jitter Measurements of Agilent Technologies OC-48 Optical Transceivers using the OmniBER718", Agilent Tech., UK, 2000.

6. P.-L. Cantin, "2.5 Gbps Links Jitter Budget; Backplane and Expansion for the PBR Rel. 1", Design Specifications Hyperchip Inc., Canada, 2001.

7. K. Droggemuller, et al., "Current Progress of Advanced High Speed Parallel Optical Links for Computer Clusters and Switching Systems", Proceedings IEEE Electronic Components and Technology Conference, 2000.

8. Y. Yang, J. Wang, "Optimal All-to-All Personalized Exchange in a Class of Optical Multistage Networks", IEEE Transactions on Parallel and Distributed Systems, Vol. 12, No. 6, June 2001.

9. L.A. Buckman et al., "Crosstalk Penalty in All-Optical Distributed Switching Networks", IEEE Photon. Tech. Letter, Vol. 9, No.2, Feb. 1997.

10. Y.-M. Wong, D. Muehlner, et al., "Technology Development of a High-Density 32-Channel 16 Gb/s Optical Data Link for Optical Interconnection Applications for the Optoelectronic Technology Consortium", Journal of Lightwave Tech., Vol. 13, No. 6, June 1995.

11. Y. Yang, J. Wang, "Optimal All-to-All Personalized Exchange in a Class of Optical Multistage Networks", IEEE Transactions on Parallel and Distributed Systems, Vol. 12, No. 6, June 2001.

12. Y. Pan, C. Qiao, Y. Yang, "Optical Multistage Interconnection Networks: New Challenges and Approaches", IEEE Comm. Magazine, Feb. 1999.

13. Q.-P. Gu, S. Peng, "Wavelength Requirements for Permutation Routing in All-Optical Multistage Interconnection Networks", 14th International Parallel and Distributed Processing Symposium, Conference Proceedings, Mexico, May 2000.

14. G. Zhou et al., "Design of Giga-Bit/s Optical Interconnection Network for Computer Cluster", Fifth International Conference on Massively Parallel Processing, Conference Proceedings, USA, 1998.

15. Y.Yang, J. Wang, Y. Pan, "Permutation Capability of Optical Multi-Stage Interconnection Networks", Parallel Processing Symposium, Proceedings of the First Merged International ... and Symposium on Parallel and Distributed Processing, Orlando, USA, April 1998.

16. H. J. Chao, T.-S. Wang, "An Optical Interconnection Network for Terabit IP Routers", Journal of Lightwave Technology, Vol. 18, No. 12, Dec. 2000.

17. L.A. Buckman et al., "A Novel All-Optical Self-Routed Wavelength-Addressable Network (SWANET)", IEEE Photon. Tech. Letter, Vol. 7, No.9, Sep. 1993.

18. L.A. Buckman et al., "Crosstalk Penalty in All-Optical Distributed Switching Networks", IEEE Photon. Tech. Letter, Vol. 9, No.2, Feb. 1997.

19. J. Zhou, R. Cadeddu, et al., "Crosstalk in Multiwavelength Optical Cross-Connect Networks", Journal of Lightwave Technology, Vol. 14, No. 6, Jun. 1996.

20. E.L. Goldstein, L. Eskildsen, "Scaling Limitations in Transparent Optical Networks Due to Low-Level Crosstalk", IEEE Photon. Tech. Letter, Vol. 7, No.1, Jan. 1993.

21. D. Jin, Q. Jiang, M. Kavehrad, "Performance Degradation Due to Crosstalk in Multiwavelength Optical Networks Using Dynamic Wavelength Routing", IEEE Photon. Tech. Lett., Vol. 7, No. 10, October 1995.

22. Y. Jin, M. Kavehrad, "An Optical Crossconnect System as a High-Speed Switching Core and Its Performance Analysis", Journal of Lightwave Technology, Vol. 14, No. 6, Jun. 1996.

23. C. Saxtoft, P. Chidgey, "Error Rate Degradation Due to Switch Crosstalk in Large Modular Switched Optical Networks", IEEE Photon. Tech. Lett., Vol. 5, No. 7, July 1993.

24. L. Gillner, C. P. Larsen, M. Gustavsson, "Scalability of Optical Multiwavelength Switching Networks: Crosstalk Analysis", Journal of Lightwave Technology, Vol. 17, No. 1, Jun. 1999.

25. E.L. Goldstein et al., "Performance Implication of Component Crosstalk in Transparent Lightwave Networks", IEEE Photon. Tech. Lett., Vol. 6, No. 5, May 1994.

26. L. Gillner, C. P. Larsen, M. Gustavsson, "Statistical Analysis of Inteferometric Crosstalk: Theory and Optical Network Example", Journal of Lightwave Technology, Vol. 15, No. 11, Nov. 1997.

Chapter 5 Experimental Set-up and Plan

This chapter describes the experimental set-up used to characterize the crosstalk of the POI described in Chapter 2. All tests were performed while operating all POI channels simultaneously. This chapter also lists some interesting experimental techniques used to measure electrical and optical crosstalk, as found in literature. Although these techniques were not used here, they are useful for testing other POI components. Note that time and budgetary constraints made it impossible to purchase a parallel BER tester. A unique test set-up was thus created to measure crosstalk. It used a dual channel BER tester, optical switches and channel driver boards developed in-house, which gave the ability to drive the 1x12 array simultaneously as well as taking readings for all 12 channels in parallel with maximum automation and minimum manipulation of the components. This set-up minimized the problems associated with keeping experimental conditions constant throughout the experimentation.

5.1 Lab set-up and Test equipment selection

5.1.1 Physical Test set-up

The experimental set-up depicted in Figure 17 was used to characterize POI crosstalk. It allowed the simultaneous measurement and control of the optical power of three adjacent channels as well as eye and BER measurements of the channel under test with a minimum of fiber manipulation during testing. It also allowed the study of eye/BER degradation due to crosstalk and its effect on system link budget.

A few modifications were added to the set-up used in [1]: 2 extra optical switches were added to minimize the total number of fiber manipulations done during the experiments. The VCSEL array was connected to a fan-out parallel optical fiber (100 meters of 62.5 μm MMF). The Channel Under Test (CUT) was connected to a variable optical attenuator or VOA (EXFO IQ-3100D-EI-EUI-91), which was then connected to an optical switch (Agilent 8606X). One of the outputs of the optical switch was sent to the corresponding channel on a fan-in cable (100 meters of 62.5 μm MMF), which was connected to the PIN array test board (the total fiber length for all channels was 204 meters). A second switch output was connected to an EXFO power meter, IQ-1643-FOA-254. Finally, the last switch output was connected to a Digital Communications Analyzer (Agilent 86100 with 86101A plug-in). The channels adjacent to the channel under test (CUT) were connected to manual VOAs, which were linked to identical optical switches. The first output of the optical switches was connected to the corresponding channels on the fan-in parallel fiber cable, which was in turn connected to the PIN array. The second output was connected to the same power meter as the CUT.

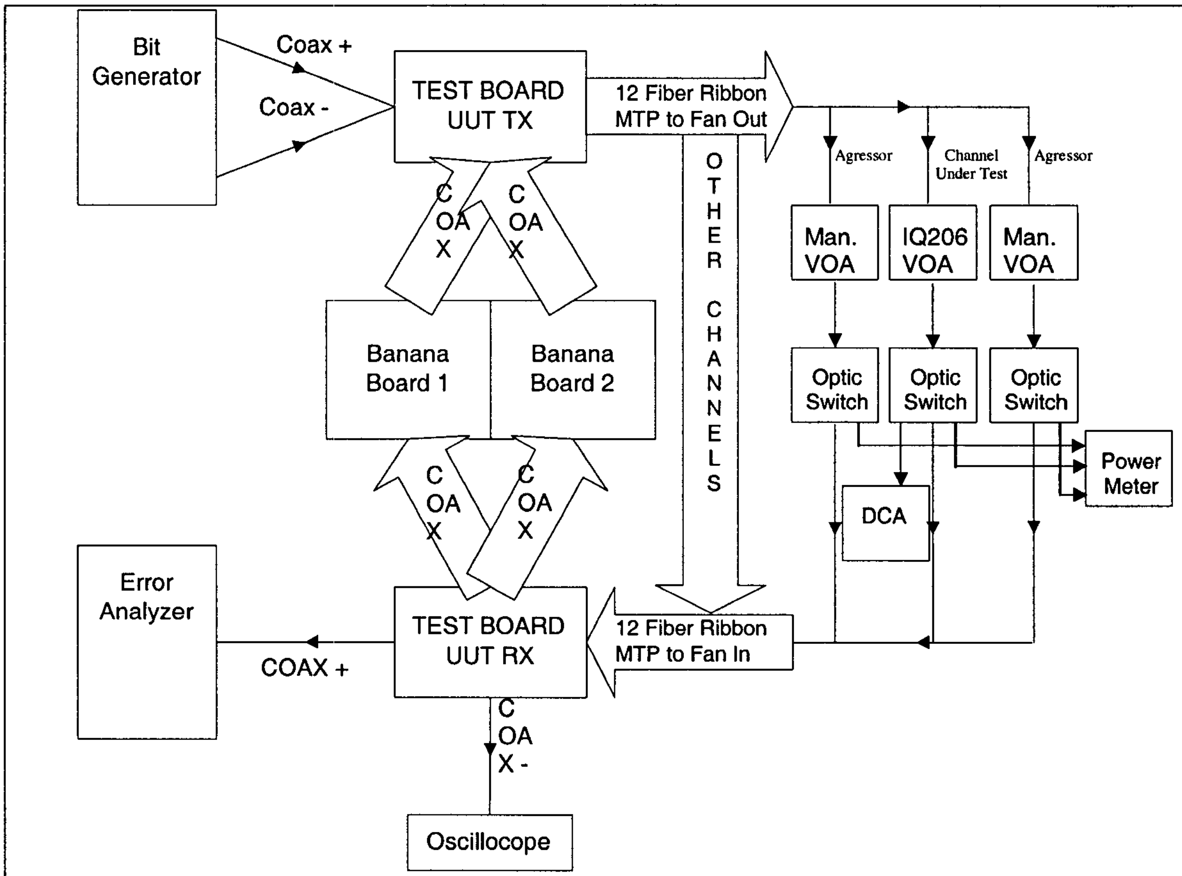

Figure 17: Diagram of test set-up for measuring POI crosstalk (multi-channel operation)

The manufacturer test boards mentioned in Chapter 2 provided an electrical interface toward the modules and are shown in Figure 6. A BER tester (Agilent 86130A) generated the input to the Tx CUT. The corresponding Rx PIN array electrical output was sent either to the same BERT (Agilent 86130A) detector section and its sampling oscilloscope (Tektronix TDS7404

TDS) to record the eye diagram and to study the significant parameters of the reconstructed waveform. The full set-up is shown in Figure 18.

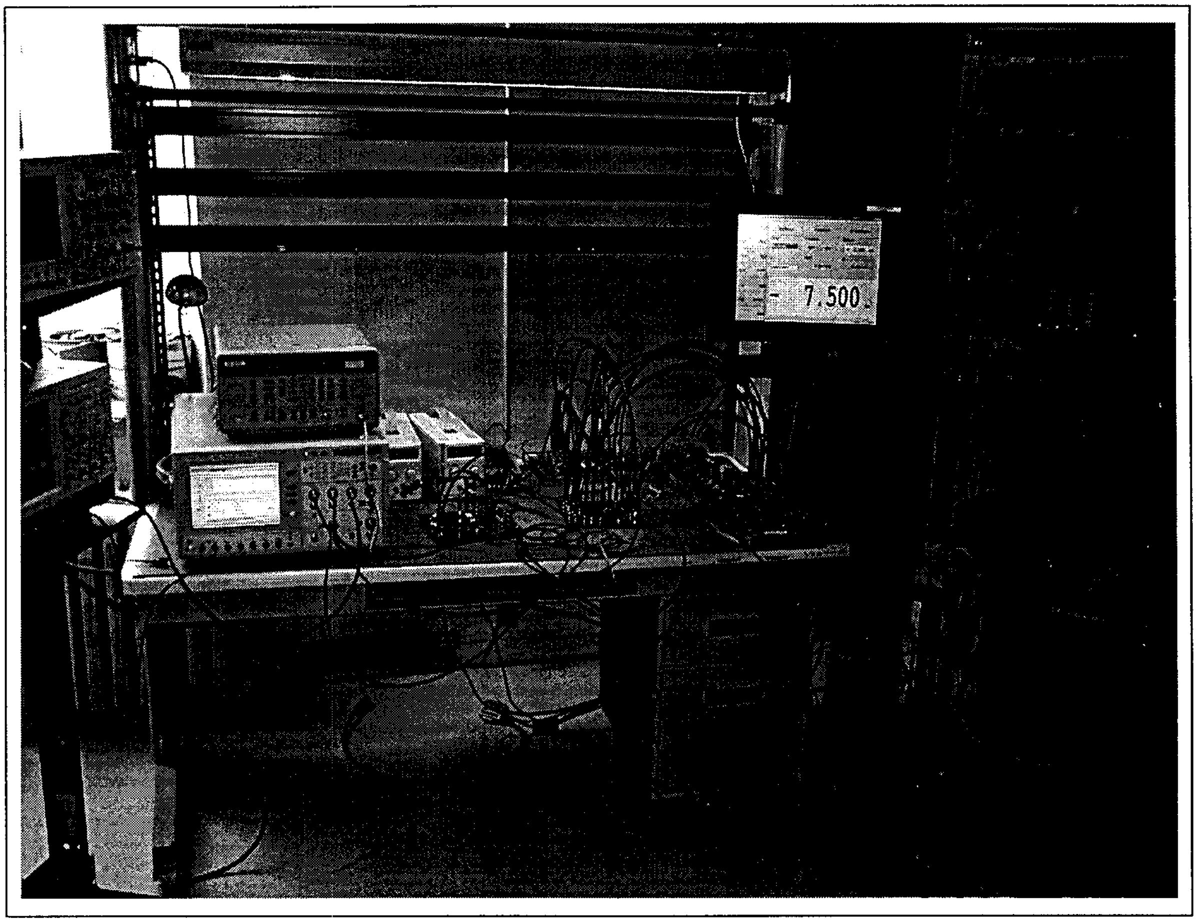

Figure 18: Test set-up for measuring POI crosstalk (multi-channel operation)

Two boards designed in-house dubbed "banana boards" and described in [1] always drive the aggressor channels of the VCSEL/PIN arrays using SMA connections. Each can drive up to 8 differential data lines simultaneously. These data lines are independent synchronous pseudo-random bit sequences (PRBS) of length 2^{23}-1 [2]. Interleaving the signals from the 2 boards ensures asynchronous behaviour between adjacent aggressor channels. Using these banana boards enable the aggressor channels to always be driven while studying the crosstalk of the CUT and provide for a more real-life operational situation.

The optical switches and VOAs added many optical connections into the optical path of the channels tested (approximately 1-2 dB extra in losses). But since we are interested in observing the variations across the array, the extra losses will appear for each channel observed. Also, these losses will worsen the results found with the 204 meters of 62.5 μm/160MHz multi-mode fiber used in this experiment. This is in-line with the "worst-case" scenario approach used in this thesis and in [1].

Finally, this set-up needed to be reconfigured for every channel being tested. Each time a CUT was changed, all the fibers and connectors were cleaned using standard fiber cleaning procedures [3]. This simulates real-life applications.

5.1.2 Statistical framework:

We used PRBS of length 2^{23}-1 and 2^{7}-1 throughout the experiments. PRBS 2^{23}-1 is the most commonly used data pattern used to simulate data transmission while PRBS 2^{7}-1 simulates data encoding used in the POI (this is more representative of real-life situations). PRBS 2^{7}-1 is also used in local area networks (LAN) using short run codes and is similar to the 8B/10B encoding used in Gigabit Ethernet [4, 5]. The data pattern was also found to have little impact on POI jitter [1] and thus it was not varied in the experiment. An average of 3 readings was taken to minimize experimental error and measurements were taken at steady state.

Because the data collection period for 10^{-12} BER was extended, 10^{-12} BER results were extrapolated from 10^{-9} BER measurements as per the method described in [1].

5.1.3 General Settings

Unless otherwise stated, all channels were driven at 2.5 Gb/s as this bit rate represents the operating bit rate of the POI. To make sure data from adjacent channels is uncorrelated and asynchronous, the connections from the 2 "banana boards" to the POI test boards were alternated.

Furthermore, for all tests, the bias voltage for the laser and Rx arrays were set at 3.3 V as prescribed by the manufacturer [6].

Finally, the ambient temperature was kept constant (approximately 20 degrees C)

5.2 Experimental Strategy

5.2.1 Experimental Techniques for Evaluating Crosstalk

When characterizing POI crosstalk, the main challenge is to differentiate between electrical and optical crosstalk. The best approaches consist of either varying the input current of the VCSEL array and observing fluctuations in the optical output power levels of the VCSELs [7] or varying the input optical power to the PIN array and measuring any fluctuations in the output current or voltage of neighboring channels [8]. Although these techniques are interesting, it was not possible to vary or monitor the bias current and voltage of the POI components in this thesis. Since the VCSEL/PIN arrays are BGA based, they did not allow for any probing of the Tx and Rx component pins for electrical current and voltage measurements.

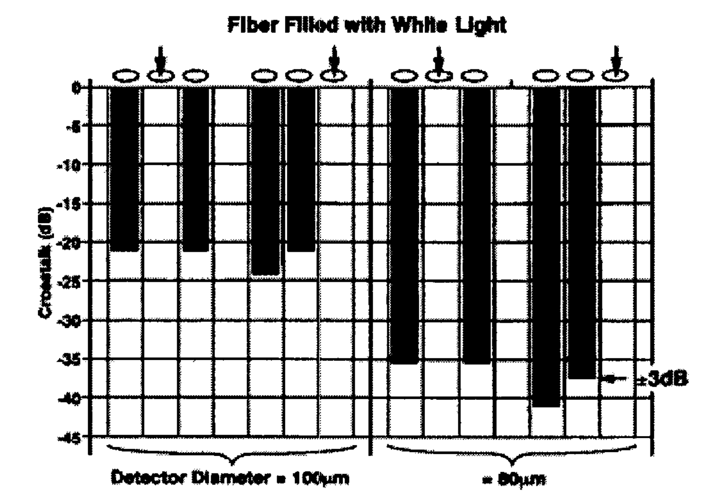

Figure 19: Results of an experiment to measure optical crosstalk [9]

We can also measure optical crosstalk by sending an optical signal to one channel and measuring the optical power on the nearest (NN) and next-nearest neighbor (NNN) channels. Only these four channels were found to impact the performance of a POI channel through optical crosstalk. The NN channels have been found to have a greater impact than the NNN channels (approximately 3 dB difference) as observed from the measurements made on a 1D 32x1 channel VCSEL array-based POI using 62.5 μm GRIN MMF [9]. The same behavior is expected from the 1-D POI tested in this thesis. In a 2-D array, the impact of the NNs and NNNs channels is expected to be worse as each channels has more neighbors. Also, as expected, the VCSELs on the periphery of an array have better SNR and waveform than those in middle of 2D array [10].

Crosstalk can be evaluated by comparing the eye opening observed when all channels are being operated to that obtained when one channel is active. The value of the penalty is estimated from the reduction in vertical eye opening, corresponding to an increased width of the logic levels. This effect on the high and low levels is also accompanied by an increase of the jitter on the rising and falling edges, which translates into a larger pulse width.

When measuring crosstalk, variations in eye patterns across channels might be due to the variation in board traceline impedance, causing signal reflection and parasitic capacitance associated with each channel [10]. However, when all devices within the array have the same characteristics, which was verified to be the case in this experiment (Chapter 2), it can be determined that the dominant contributor to performance degradation is crosstalk.

5.2.2 Experimental Test-Plan

The experiment was divided into 2 sets of experiment: the first set analyzed the basic components of POI performance, and aimed to determine the performance limits of the POI. Part of this work was done in conjunction with [1]. The second set of measurements focused specifically on isolating the possible sources of the performance degradation identified in the first set of general measurements, within the POI itself (Tx, Rx, fiber, connectors) and determining the major crosstalk contributor, i.e. electrical or optical.

The BER and jitter measuring techniques described in Chapter 4 were used in this experiment. Also, the data collection was automated using the LabView program detailed in [1]. A general description of these tests and their goals follows.

5.2.2.1 General Characterization of POI Crosstalk

The different tests performed to obtain the basic characteristics of the POI operation are listed below:

1. **Wavelength Measurements:**

    a. **Goal**: to determine the transmission wavelength of each channel. The information collected here can help determine if optical crosstalk is homodyne or heterodyne. If the wavelength variation is large, then this information can be used to characterize the source of optical crosstalk at the Tx end.

b. **Procedure**: using the set-up of Figure 17 while driving all channels simultaneously, the output of optical switch #2 is connected to an optical spectrum analyzer Advantest Q8384, where the actual wavelength of the channels is measured.

2. **Optical output power of VCSEL array channels when channels are not being driven:**

    a. **Goal:** to determine if single channel operation is affected by the non-operation of adjacent channels and performance uniformity across channels.

    b. **Procedure**: with the Tx modules biased at 3.3 V, but not connected to the driver boards, measure the output optical power of each individual channel with the power meter.

3. **Optical output power of VCSEL array channels when channels are being driven:**

    a. **Goal:** to determine the output power of all channels when operated in multi-channel configuration and to determine the uniformity of performance across all channels; to determine if there is a difference with the results of test #2)

    b. **Procedure**: same as test #2b) but with the Tx and Rx modules connected to the driver boards to drive all channels adjacent to the CUT.

4. **Rx Power uniformity- 0 aggressor channels:**

    a. **Goal:** to determine the BER changes with variation in maximum receive optical power across all 12 channels when no other channel is in operation, and to identify the uniformity of performance across all channels.

    b. **Procedure**: drive each channel individually and perform a waterfall curve measurement for each channel as per the technique described in [1].

5. **Rx Power uniformity- 11 aggressor channels:**

a. **Goal:** to determine the changes in BER with variation in maximum receive optical power across all 12 channels when all the other channels are in operation, and to identify the uniformity of performance across all channels.

b. **Procedure**: drive all channels simultaneously using the driver boards and perform a waterfall curve measurement for each channel as per the technique described in [1].

5.2.2.2 Crosstalk Characterization of Individual POI Components

The tests performed to isolate the sources of crosstalk within the POI and to determine the cause of this crosstalk are listed below:

1. **Cross-talk characterization of fiber medium:**

   a. **Goal**: to determine if optical crosstalk within the fiber medium exists and to quickly verify the supplier specifications.

   b. **Procedure**: this test is done by simply lighting up one channel of the parallel fiber cable and measuring optical output power on adjacent channels.

2. **BER and Eye Opening Penalty due to optical crosstalk at the Tx side:**

   a. **Goal**: to determine the BER penalty and eye opening penalty due to optical crosstalk leakage in both the Tx and the Rx modules, to determine how many adjacent channels will impact BER and eye opening performance and to determine the performance uniformity across the entire array.

   b. **Procedure**:

      This test is done in 2 parts:

      i. When driving the CUT, aggressor channels are added or removed progressively and changes in the CUT BER, ER, and eye pattern are observed at the receive end

ii. The output of the Tx module is fed directly in the DCA and aggressor channels is added or removed progressively: changes in the CUT BER and eye pattern are observed at the transmit end

3. **Characterization of Rx Crosstalk**

   a. **Goal**: to determine the impact of optical crosstalk on Rx performance

   b. **Procedure**:

This test is done in 2 parts:

i. Using the set-up in Figure 18, waterfall curves are obtained for the different CUT while maintaining the difference between the optical power of the adjacent channels and the CUT constant. This is achieved by manually setting the variable optical attenuators of the nearest neighbor channels to the right attenuation level.

ii. As shown in Figure 20 below, a completely different Tx module is used to send light to the Rx channels adjacent to the CUT. By using a different Tx module, to provide the optical power of the aggressor channels, we isolate the receive end of the CUT and can determine if optical crosstalk contributions from the aggressor channels impact CUT BER. In this case, a Picolight 12x2.5 Gb/s VCSEL array, (Part# PL-TCP-00-S53-0B) is used because it was available. Any other similar VCSEL array based laser could have been used as variations in receiver BER are observed. Two Picolight channels are connected to the fiber channels in the fiber ribbon array that are as far away from the channel under test as possible. At the receive end, these aggressor channels are connected to the nearest neighbors of the CUT. This can be achieved using a fan-out fiber ribbon at the Tx side and a fan-in fiber ribbon at the Rx end.

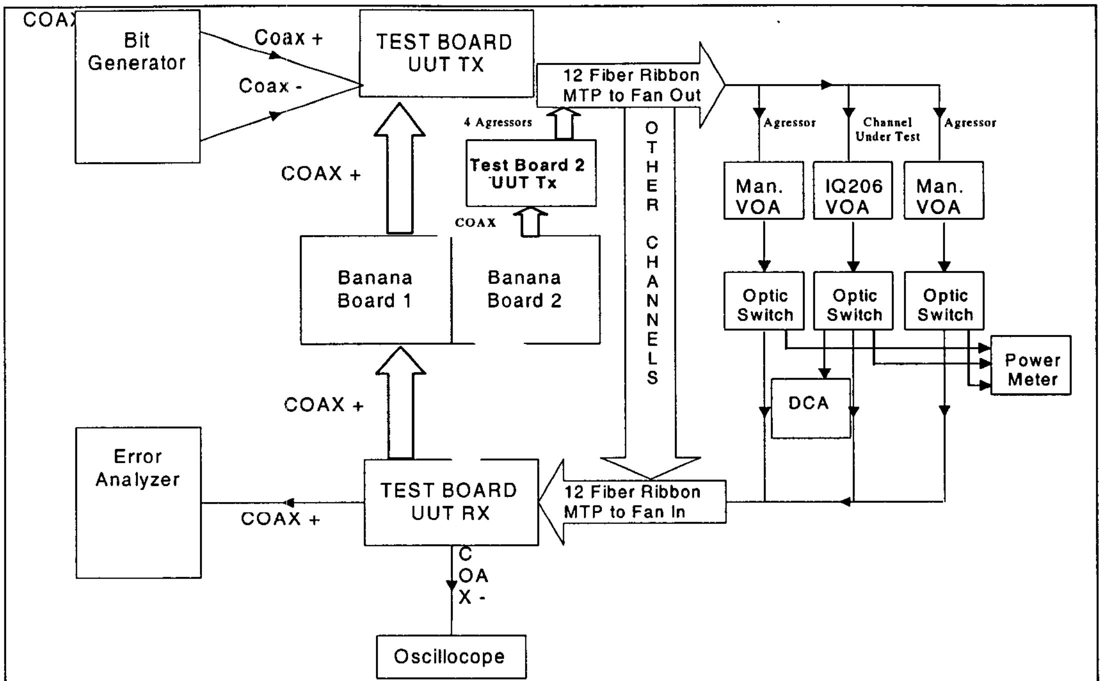

Figure 20: Experimental set-up to measure optical crosstalk at the receive end of a POI

4. **Impact of cross talk on POI jitter performance**

    a. **Goal**: to determine the tolerance of the POI to jitter performance degradation with multi-channel operation.

    b. **Procedure**: The "Rx Power uniformity- 0 aggressor channels" and "Rx Power uniformity- 11 aggressor channels" procedures are repeated but jitter was measured instead using the bathtub curve method described previously.

5.3 Summary

The unique test setup and testing methodology designed to characterize POI crosstalk was described in this chapter. The set-up minimized component manipulation throughout the testing of the POI. Industry standard component handling procedures were followed whenever components needed to be handled.

5.4 References

1. M. Salzberg, "Testing and Characterization of a Parallel Optical Interconnect for a Scalable Routing System" Master's thesis, McGill University, 2001.

2. O. Hebert, "Banana Board FPGA 'Chiquita' Design Specification", Hyperchip Inc., Canada, 2001

3. F. Guevin, "Fiber Cleaning Procedure", Hyperchip Inc., Canada, 2001.

4. L. B. Aronson, B. E. Lemoff, L.A. Buckman, D. W. Dolfi, "Low-Cost Multimode WDM for Local Area Networks Up to 10 Gb/s", IEEE Photon. Tech. Lett., Vol. 10, No. 10, Oct. 1998.].

5. L.A. Buckman et al., "Crosstalk Penalty in All-Optical Distributed Switching Networks", IEEE Photon. Tech. Letter, Vol. 9, No.2, Feb. 1997.

6. Agilent Technologies, "Agilent HFBR-712BP and HFBR-722BP Parallel Fiber Optic Modules – 850nm VCSEL Array Transmitter and Receiver 1 to 2.5 GBd per channel", Preliminary Data Sheet, USA, August 2001.

7. G. Heise, "Crosstalk Investigation of Laser-Diode Pairs", IEEE Photon. Tech. Letters, Vol. 2, No. 2, Feb. 1990

8. S. Nakagawa, S. -Y. Hu, D. Louderback, L. A. Coldren, "RF Crosstalk in Multi-Wavelength Vertical-Cavity Surface-Emitting Laser Arrays", IEEE Photon. Tech. Lett., Vol. 12, No. 6, June 2000.

9. Y.-M. Wong, D. Muehlner, et al., "Technology Development of a High-Density 32-Channel 16 Gb/s Optical Data Link for Optical Interconnection Applications for the Optoelectronic Technology Consortium", Journal of Lightwave Tech., Vol. 13, No. 6, June 1995.

10. Nam-Hyong Kim, "2-D Free-Space Optical Backplane Using Vertical Cavity Surface Emitting Laser", Master's Thesis, Department of Electrical Engineering, McGill University, Montreal, Canada, July 1996.

Chapter 6

Experimental Results and Impact on System Performance

Test results obtained from all experiments described in Chapter 5 are explained in this chapter. Observations and experimental analysis are also included.

6.1 Experimental results

6.1.1 General Characterization

6.1.1.1 Wavelength Measurements

The measured channel wavelengths varied by less than one nanometer across the 12-channel POI array (Figure 21). The average wavelength was 845.4 nm with standard deviation of 0.08 nm. This represents excellent uniformity across the array. Hence, it was not possible to use wavelength as a "marker" for identifying the possible source of optical crosstalk. These results also confirm that if the there is optical crosstalk caused by the Tx module, it will be of homodyne nature since the all the wavelengths center around 845 nm.

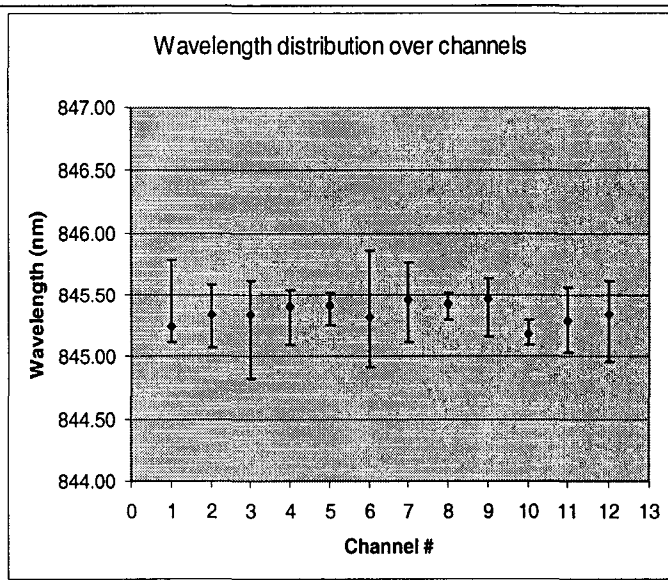

Figure 21: Channel wavelengths

6.1.1.2 Launch Optical Power (no connections to the driver boards)

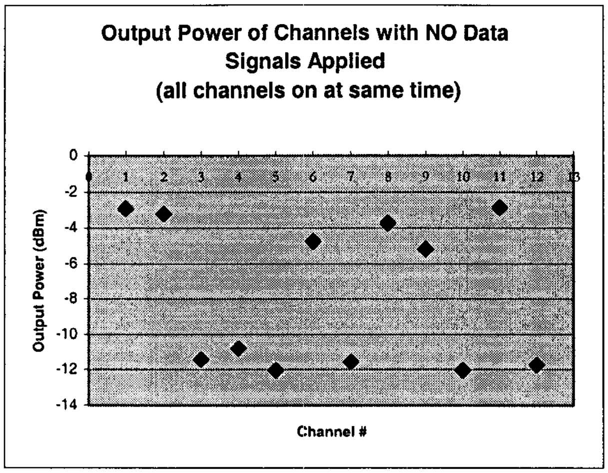

Figure 22: Optical transmit power per channel (bias only)

The results shown in Figure 22 show an interesting phenomenon: when the Tx module is biased at 3.3V but is not connected to the "banana" boards, the Tx channels still generate optical power, in some cases as high as –3 dBm. The high optical power of these channels can impact the performance of any channel being tested, which means that when characterizing POI crosstalk, only the aggressor channels that are being driven with the driver boards are connected optically to the fiber ribbon(s). Any Tx channel that is not being driven is not connected optically to minimize potential crosstalk noise due to the high optical output power as observed in Figure 22. The output power varied randomly across the array. It was recommended to squelch the optical output power of un-driven channels to POI component suppliers.

6.1.1.3 Launch optical power drive

Optical launch power measurements were made in [1] and repeated below in Figure 23. The bias voltage is varied within the limits prescribed by the manufacturer [2] to determine the sensitivity of the Tx module to variations in power supply voltage. As expected, the output optical power varied little when the bias voltage of the Tx module was varied within specifications. Furthermore, the channel-to-channel variation was small, with a standard deviation of 0.21 dB for an average Tx optical power of – 3.91 dBm. The optical launch power was found to be insensitive to signal pattern. This corroborates the findings in [1].

The optical output power was found to be independent of bit rate. The output optical power measured at a bit rate of 2.125 Gb/s was almost identical to that measured at 2.5 Gb/s [1], as shown in Figure 23 and Figure 24. These latter measurements will be most significant for O-MIN applications where an increase in bit rate beyond 2.5 Gb/s is planned without requiring any changes in the installed fiber plant.

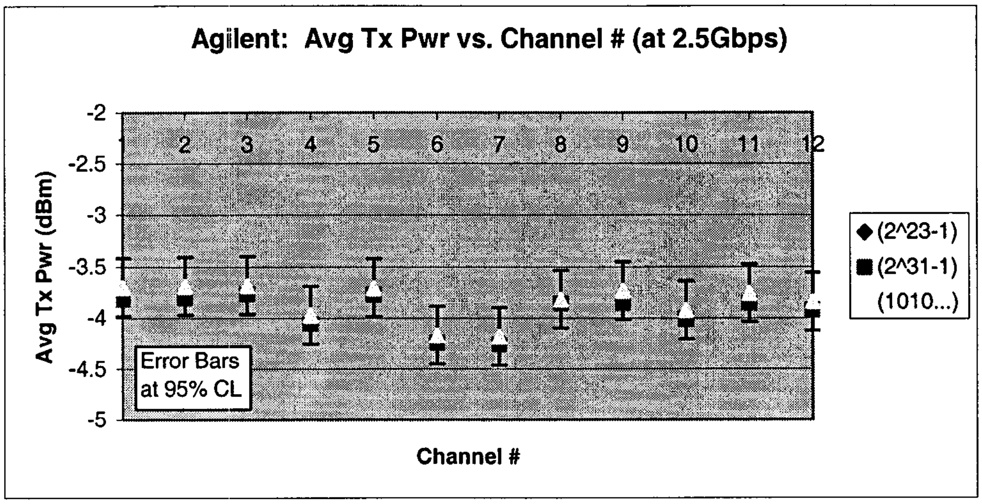

Figure 23: Optical output power per channel (2.5 Gb/s) [1]

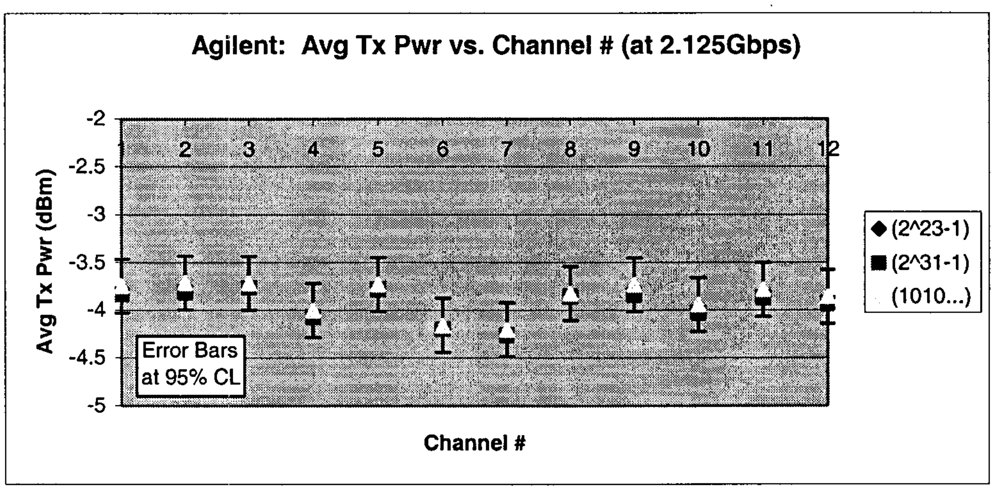

Figure 24: Optical output power per channel (2.125 Gb/s)

6.1.1.4 Single-Channel and Multi-Channel Testing

Figure 25 plots single-channel operation together with multi-channel operation of the POI in order to get a good estimation of the power penalty associated with the multi-channel operation of each channel of the POI with the 204-meter fiber ribbon link described in 5.1.1. Multi-channel operation includes the operation of all 12 POI channels simultaneously. The observed power penalties at BER of 10^{-12} are shown explicitly in Table 6. To ensure the validity of the experimental data, 2 sets of measurements were completed separately for the single channel operation and the multi-channel operation.

Channel	1	2	3	4	5	6	7	8	9	10	11	12
Power Penalty (dB)	3.5	5.3	4.2	5.1	5.6	4.6	5.8	4.3	5.0	5.2	4.9	3.9

Table 6: Measured power penalty per channel for multi-channel operation at 2.5 Gb/s and a 10^{-12} BER

As expected the power penalty is smallest at the edge of the POI, i.e. on channels 1 and 12 since these channels have less neighbors than the other channels. Also the middle channels have the highest penalty. The average power penalty averages across the array is 4.8 dB, which is significant. The standard deviation is 0.7 dB, which shows a fairly consistent penalty across the array. For link budgeting purposes, the worst-case penalty should be used, corresponding to a reduction of 5.8 dB relative to the average single channel case. This observed power penalty is due to crosstalk at either the Tx or Rx ends, or at both ends and subsequent testing in this chapter will aim to pinpoint the exact source.

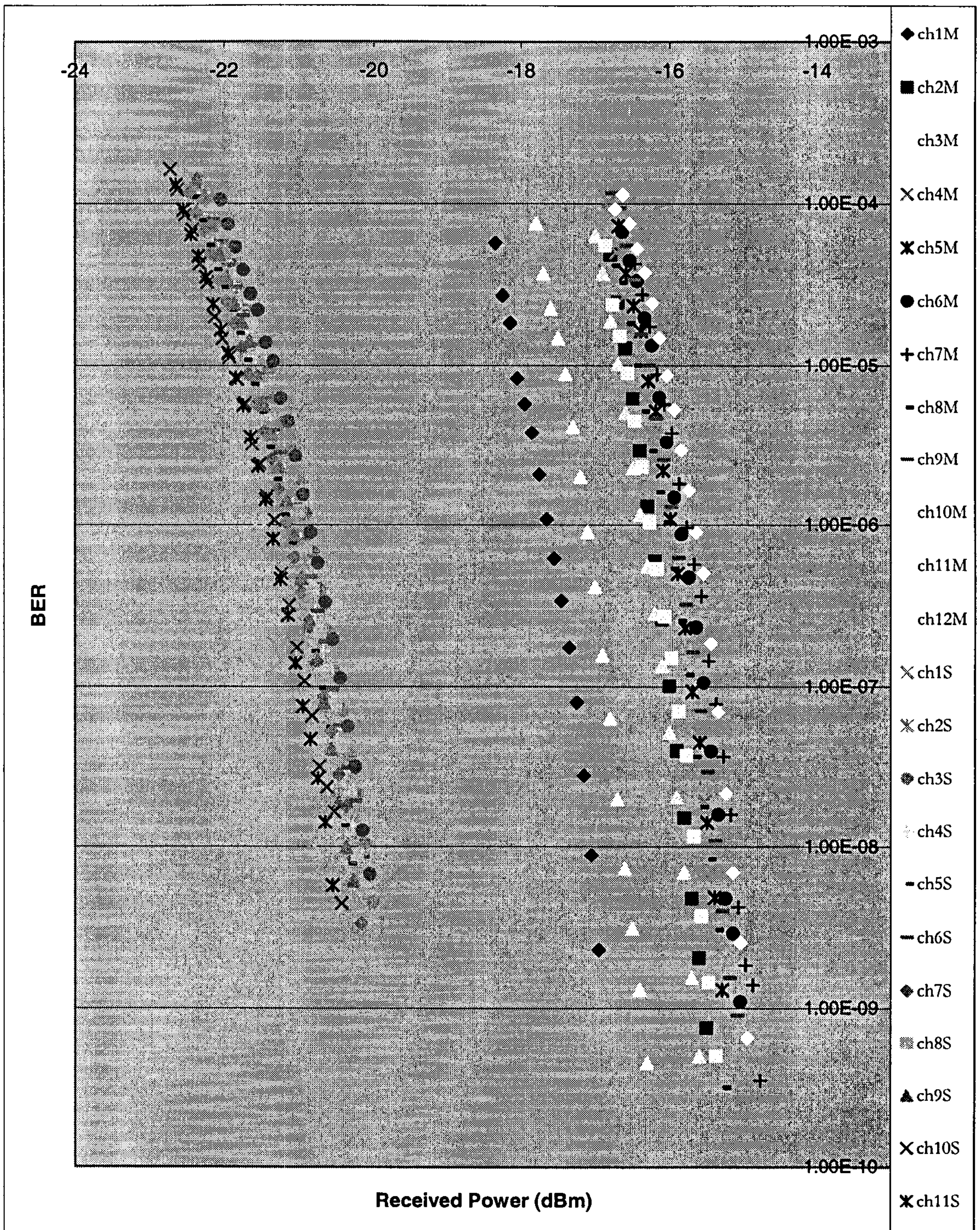

Figure 25: BER versus Rx power for single channel and multi-channel operation at 2.5 Gb/s (crosstalk power penalty)—M=Multi-channel operation and S=single channel operation

The steepness of the waterfall curves collected in Figure 25 is expected, as it is typical of optical receivers. Hence, varying the optical power by a small amount can create a radical improvement in the corresponding BER performance, i.e. from a 10^{-5} BER to a 10^{-9} BER. For example, when varying the optical power of channel #2 by 1.2 dB the BER improves from 10^{-5} to a 10^{-9} during the waterfall curve measurements, as shown in the experimental results listed in Table 7 below.

DATA:

Waterfall Curves for Multi-Channel CH2				Step (dB)
-				0.1
Power @ PM (dBm)	**VOA settings (dB)**	**Pass 1**	**Pass 2**	**Average**
-16.8	-9.8	5.00E-05	4.70E-05	4.85E-05
-16.7	-9.7	2.45E-05	2.48E-05	2.47E-05
-16.6	-9.6	1.26E-05	1.30E-05	1.28E-05
-16.5	-9.5	6.20E-06	6.30E-06	6.25E-06
-16.4	-9.4	2.86E-06	2.98E-06	2.92E-06
-16.3	-9.3	1.32E-06	1.29E-06	1.31E-06
-16.2	-9.2	6.10E-07	5.80E-07	5.95E-07
-16.1	-9.1	2.63E-07	2.60E-07	2.62E-07
-16	-9	9.60E-08	1.06E-07	1.01E-07
-15.9	-8.9	3.80E-08	4.20E-08	4.00E-08
-15.8	-8.8	1.53E-08	1.50E-08	1.52E-08
-15.7	-8.7	5.20E-09	4.30E-09	4.75E-09
-15.6	-8.6	2.30E-09	1.80E-09	2.05E-09
-15.5	-8.5	7.00E-10	8.00E-10	7.50E-10

Table 7: Waterfall curve measurements for channel #2 (multi-channel operation at 2.5 Gb/s)

Table 8 summarizes the maximum power variation needed to obtain the same BER improvements. The channel performance is consistent across the array (standard deviation of 0.15 dB).

Channel	1	2	3	4	5	6	7	8	9	10	11	12
Optical Power Δ (dB)	1.4	1.3	1.4	1.5	1.4	1.6	1.7	1.5	1.7	1.8	1.5	1.5

Table 8: Optical power variation across channels (multi-channel operation at 2.5 Gb/s)

The results in Table 8 indicate that performance of all channels within the POI array are sensitive to variations of less than 2 dB when operated in multi-channel fashion. However, these power penalties represented absolute worst-case scenarios since only the received power of the CUT was attenuated relative to the full optical power of the aggressor channels. Therefore the worst-case 5.8 dB power penalty listed in Table 6 previously will have to be adjusted to reflect a more real-life application as will be seen later in this chapter.

Large variations in Rx sensitivities are also observed in multi-channel operation. These Rx sensitivities are listed in Table 9: the average sensitivity for a 10^{-12} BER is –14.8 dBm with a maximum deviation of 2.3 dB and a standard deviation of 0.6 dB. The average receive power is –19.7 dBm and the standard deviation falls to 0.3 dB for single-channel operation.

Channel	1	2	3	4	5	6	7	8	9	10	11	12
Rx Sensitivity (dBm)	-16.4	-14.7	-15.2	-14.8	-14.6	-14.5	-14.1	-15	-14.4	-14.5	-15.1	-15.4

Table 9: Receive power per channel for 10^{-12} BER (multi-channel operation)

The measured Rx sensitivities at 10^{-12} BER are greater than the -16 dBm prescribed by the component vendor [2]. This is because the components used in the experiment were early prototypes. However it will be important to get assurance from the component vendors that the parts used in real-life applications meet the prescribed Rx sensitivity [5].

These Rx sensitivity and multi-channel operation power penalties translate into a worst-case 9.8 dB link budget as shown in Table 10. The maximum link budget variation between channels is 2.85 dB, which can affect the scalability of a multi-hop O-MIN as will be discussed later in this chapter.

Channel	1	2	3	4	5	6	7	8	9	10	11	12
Link Budget (dB) 10^{-12} BER	12.65	10.95	11.5	10.7	10.9	10.25	9.8	11.15	10.6	10.5	11.3	11.45

Table 10: Per channel operational link budgets (multi-channel operation at 2.5 Gb/s)

The POI was also found to be sensitive to both bit rate and bias voltage. Waterfall curves were produced for 3 channels (Figure 26) and we observed a power penalty of up to 0.9 dB at 10^{-12} BER when the bit rate varied from 2.125 Gb/s to 3.125 Gb/s. Note that the POI was operated under multi-channel conditions. As expected from Chapter 4, there is a power penalty due to a 1 Gb/s bit rate increase and a 9% variation is rather large when compared to the average link budget of the system.

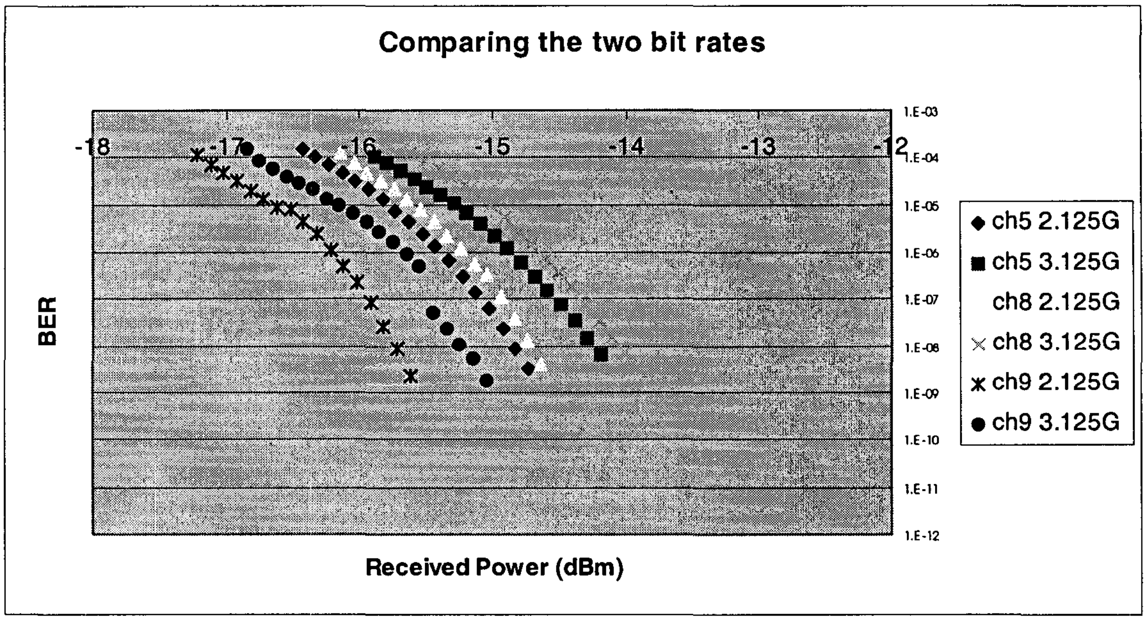

Figure 26: Waterfall curves for channels 5, 8 and 9 with bit rates of 2.125 Gb/s and 3.125 Gb/s

The channels were then operated under single and multi-channel conditions with varying bit rate in order to better understand the corresponding power penalty due to the combined effect of multi-channel operation and increased bit rate. The bit rate was only increased from 2.5 Gb/s to 3.125 Gb/s to represent a more real-life application. The experimental results are shown in Figure 27. Penalties as high as 7 dB for a BER of 10^{-12} were observed when comparing multi-channel operation with single channel (refer to channel 2 in Figure 27). However, when considering multi-channel operation only, the power penalty was less than 0.3 dB for a 10^{-12} BER when increasing the bit rate from 2.5 Gb/s to 3.125 Gb/s for both channels shown in Figure 27. Of importance is the variation in Rx sensitivity between the 2 channels below, which is approximately 1.5 dB for both 2.5 Gb/s and 3.125 Gb/s. It is interesting to note that optical power variations due to changes in bit rate are small at the Tx end (as found in section 6.1.1.3). The performance of the Rx end of the POI is thus assumed to be the major contributor to the bit rate induced BER penalty found above.

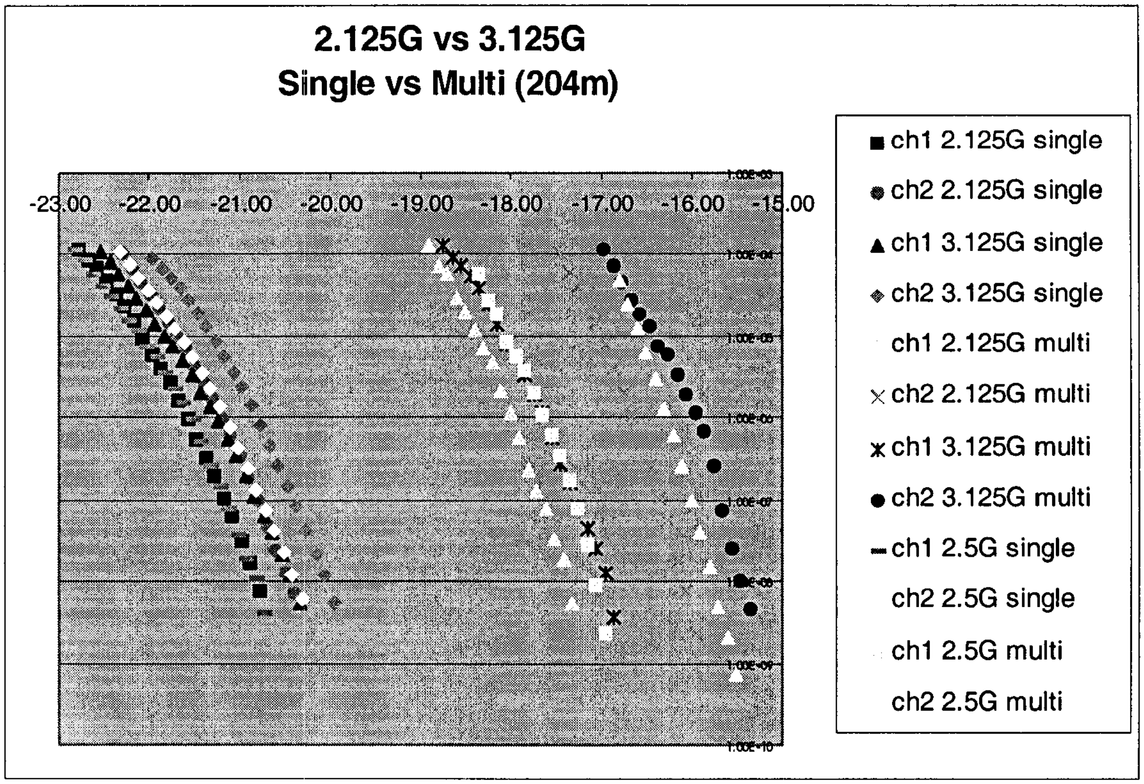

Figure 27: Graph of BER versus receive power for single and multi-channel operation at bit rates of 2.125 GB/s and 3/125 Gb/s (power penalty)

Finally, a power penalty was also observed when the bias voltage of both Tx and Rx components was varied within the limit voltages prescribed by the component vendor [2] for multi-channel operation mode. This penalty was smaller than 0.5 dB as shown in Figure 28 but still forced careful monitoring of the bias voltage throughout the experiments in order to get as accurate data as possible and ensure consistency of the experimental results.

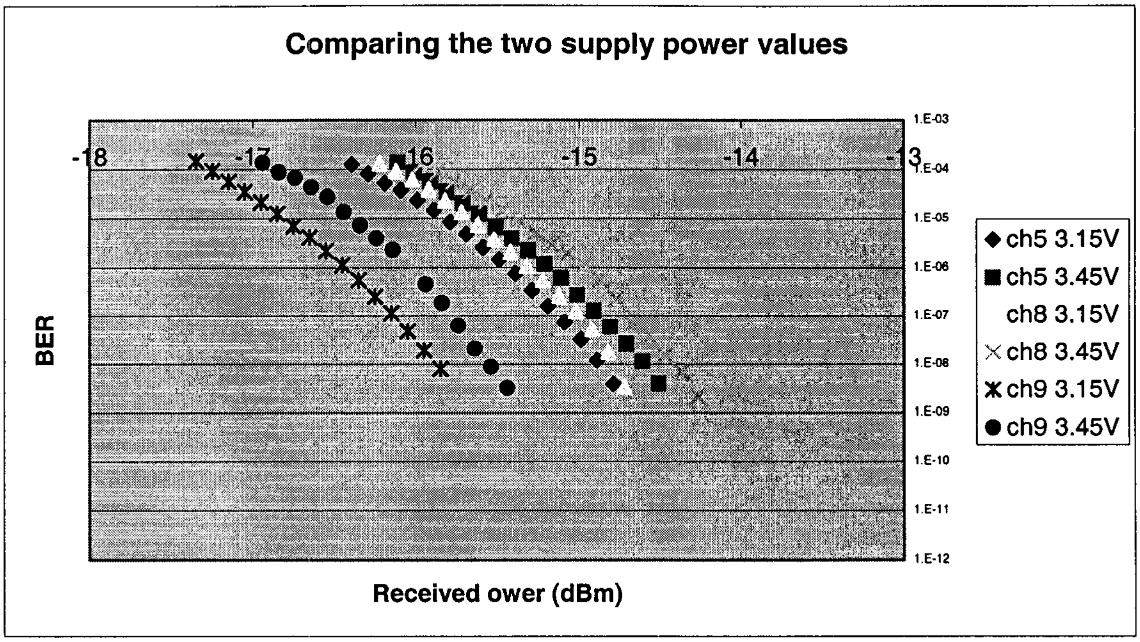

Figure 28: Graph of BER versus receive power for channels 5, 8 and 9 and bias voltages of 3.15 and 3.45 V

6.1.2 Crosstalk Characterization of Individual POI Components

The next series of experiments aimed at identifying the sources of the previously found power penalty.

6.1.2.1 Cross-talk characterization of fiber medium

This was a quick test to verify the manufacturer's claim of negligible crosstalk between fibers. The MTP connectors created a challenge when trying to isolate a single channel in the fiber ribbon cable. To make sure the true ribbon crosstalk was measured, it was necessary to block-off any crosstalk occurring at the Tx end of the POI. Therefore a fan-out cable was connected to a fan-in cable to isolate a single optical signal. This signal was then fed into a ribbon cable. Optical power was measured on channels adjacent to the lit CUT. As expected, no optical crosstalk was detected on the nearest and next-nearest neighbors with the optical power meter, which was capable of detecting weak optical signals of –85 dBm. It can therefore be concluded that optical crosstalk due to inter-channel coupling within the fiber ribbon array is negligible as it is less than –85 dBm.

6.1.2.2 BER and Eye Opening Penalty due to optical crosstalk at the Tx side:

1. Determining which aggressor channels have significant impact

The first set of experiments aimed at determining which adjacent channels has an impact on the POI performance when operating in multi-channel mode. Knowing which adjacent channels influence the CUT performance reduces the total number of tests required.

Initially, one channel was operated and driven at 2.5 Gb/s with the "banana" board while the receive power was set so a 10^{-9} BER using the variable optical attenuator. Aggressor channels were added one by one and the BER was measured. BER degraded very quickly as soon as one NN channel was added and it was not possible to determine if channels other than the nearest and next-nearest neighbors had an impact on the BER performance of the CUT. The testing strategy was thus reversed, i.e. the CUT was initially operated in multi-channel mode while its receive power was set to a low BER of 10^{-4}. This low BER was selected because it reduced the data collection period needed on the BERT and it maximized the impact of removing adjacent channels on CUT performance. The aggressor channels furthest from the CUT were disconnected one by one, first optically, by removing the fiber connection, and then electrically, by disconnecting the driver board. Channels furthest from the CUT were first disconnected, and then the next furthest channels, and so on, getting closer and closer to the CUT, until an improvement in BER was observed. Using this last technique, we were able to determine that only the nearest neighbors were found to affect CUT performance and not the next-nearest neighbors when operating a particular CUT under normal operating conditions, i.e. with no optical attenuation on the adjacent channels. Results for channel #5 are shown as an example in Table 11 below. Only results for the nearest-neighbors channels are shown since the simultaneous operation of other channels had no effect on the CUT BER.

It is interesting that both the optical and electrical connection had an impact on the BER reduction of the CUT. This is an indication that both optical and electrical crosstalk affect the BER performance of the CUT. We note that the optical transmit power varied by less than 2% when the adjacent channels were disconnected electrically from the driver boards. This indicates that the optical crosstalk did not occur at the transmit end of the POI but rather at the receive end. This will be verified later in this chapter.

Channel #5 = CUT		
Remove Channel #6	**BER**	**Tx Optical Power (dBm)**
a) electrical & optical	2.97 E-4	-17.8
b) remove optical conn.	1.29 E-6	-17.5
c) remove electrical conn.	4.46 E-7	-17.8
Remove Channel #4	**BER**	**Tx Optical Power (dBm)**
a) electrical & optical	6.62 E –7	-17.81
b) remove optical conn.	<10E-12	-17.83
c) remove electrical conn.	<10E-12	-17.79

Table 11: Test Results showing the impact of nearest-neighbour channels on the channel-under-test BER

The fact that the nearest-neighbor channel has the most impact on BER performance of the CUT is a characteristic of the POI used in this thesis. It cannot be concluded that all POI will behave in a similar manner. Nevertheless the experimental procedure described above can be used for any other POI and is a quick and easy way to determine which aggressor channel(s) will influence the CUT performance.

2. BER and Eye Opening Penalty due to optical crosstalk at the Tx side

The second set of experimental tests consisted in measuring the characteristics of the Tx channels and observing variations for multi-channel operation relative to single-channel operation. As an example, with the set-up described section 5.1, the eye pattern of channel #5 was measured using the DCA. Its optical power was also measured. When adjacent channels were connected, negligible variations in eye pattern and optical output power were measured, i.e. less than 3%. First the nearest neighbor channels were connected up and then the next-nearest neighbors. Results for 4 channels are shown below (Table 12) and include an edge channel as well as a middle-of-the array channel. These results show that behavior is the same irrespective of channel position within the array. All results were taken for a 10^{-9} BER, which was first set using the variable optical attenuator on the CUT. Then, with the optical switch, the signal was fed to the DCA.

	Optical Power (dBm)	**Jitter (ps)**
Channel # 9 (no aggressor)	-15.29	11.5
Channel #9 + NN channels	-15.28	11.2
Channel #9 + NN & NNN channels	-15.23	11.2
Channel # 2 (no aggressor)	-15.88	14.9
Channel #2+ NN channels	-15.86	14.5
Channel #2 + NN & NNN channels	-15.85	14.7
Channel # 6 (no aggressor)	-15.43	11.3
Channel #6 + NN channels	-15.46	11.0
Channel #6 + NN & NNN channels	-15.45	11.3
Channel # 10 (no aggressor)	-16.69	11.5
Channel #10 + NN channels	-16.70	11.3
Channel #10+NN & NNN channels	-16.72	11.3

Table 12: Optical crosstalk measurements on Tx side of POI

It was not possible to block-off the adjacent optical channels in the MTP connector on the Tx side without damaging the components, and thus it was not possible to determine if crosstalk occurred within the VCSEL itself, either through electrical crosstalk or through spontaneous emission coupling. Also, it would have blocked off any of the high-powered biased emissions measured in section 6.1.1.2, which might have added to the optical crosstalk due to inefficient coupling of the output transmit power. Because the variations in transmit signal parameters were negligible, it can be concluded that optical and electrical crosstalk due to the Tx module is negligible.

This means that if the present Tx module is used in an O-MIN architecture, its optical signal will not be degraded due to optical crosstalk prior to its entry in an optical redirection box. Only the inherent crosstalk associated with the optical redirection boxes will need to be considered when assessing its impact on the optical link performance, which will determine the scalability of the O-MIN.

6.1.2.3 Optical crosstalk at the Rx End of the POI:

Since it was determined there is negligible crosstalk contributions from the transmit side of the POI and the optical fiber ribbon array, it is also assumed that the crosstalk penalty observed in the first section of this chapter is due solely to Rx crosstalk, both electrical and optical. Because the Rx array was BGA-based and did not allow any probing of the array pins for electrical current variation, it was difficult to determine the extent of the electrical component of the Rx crosstalk. Therefore an estimation of the impact of optical crosstalk on the receive end is determined.

1. Characterization of Rx Crosstalk

To characterize the crosstalk induced at the Rx end, experiments were done using the set-ups described in Figure 17 and Figure 20. Because the power penalties found in section 6.1.1.4 represented cases where the optical power differences between the CUT and aggressor channels varied, two tests were performed where the difference in optical power between the CUT and the aggressor channels remained constant. To achieve this, the optical power in the aggressor channels was adjusted manually using the optical attenuators and relative to the attenuation done on the CUT. In this manner, the difference in optical power between the adjacent channels and the CUT remained constant throughout the collection of data points needed for the waterfall curves. Results for 2 channels are summarized in Figure 29 and Figure 30 below.

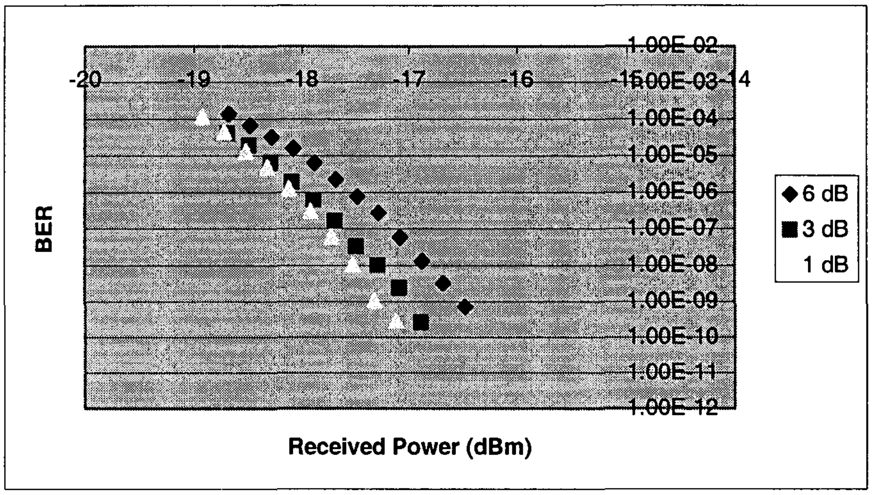

Figure 29: Graph of BER versus Rx sensitivity for channel 11 at 2.5 Gb/s (different optical power in the two nearest-neighbours channels)

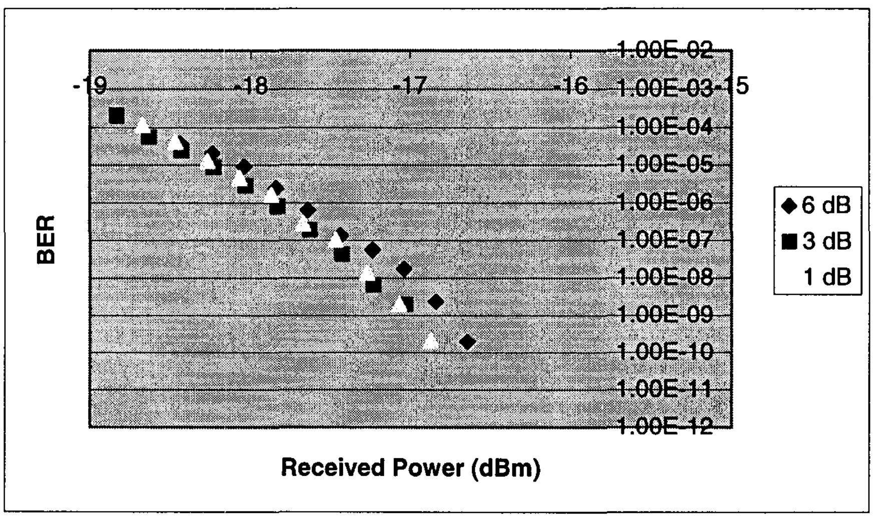

Figure 30: Graph of BER versus Rx sensitivity for channel 8 at 2.5 Gb/s (different optical power in the two nearest-neighbours channels)

As can be seen from the readings of the above two channels, the power penalty associated with an increase in optical power in the adjacent channels, relative to the optical power in the CUT is not constant: for channel 11, the power penalty is approximately 1 dB while for channel 8 it is less than 0.5 dB at 10^{-12} BER. The same is true for the other channels and the power penalty observed is less than 2 dB across all channels. We can only conclude that the impact of an increase in adjacent channel optical power relative to the CUT is not strong. It cannot be determined if the crosstalk is electrical or optical but it is suspected that it is mostly electrical following the calculations done in section 3.1.1.1.

Table 13 shows how the power penalties found in Figure 29 and Figure 30 differ from those found in Table 6 and Figure 25. Approximately 1.2 dB improvement is observed when maintaining the optical power difference between the aggressors and the CUT at 6 dB. The best improvement is less than 2 dB for an optical power difference of 1 dB. The key question becomes, what is the "pain threshold", i.e. at what is the optical power difference between channels that will impact BER significantly. This will be examined next.

Channel	**Full Power (dB)**	**Δ = 6 dB (dB)**	**Δ = 3 dB (dB)**	**Δ = 1 dB (dB)**
8	4.85	3.47	3.07	3.04
11	5.17	4.06	3.65	3.42

Table 13: Power penalties for different optical power in nearest-neighbour aggressor channels

In the second experiment, the procedure described in Figure 20 was performed with a different laser altogether to send light to channels adjacent to the CUT in the Rx module. Only the nearest neighbor channels are used since they are the only channels affecting CUT performance (as found previously in section 6.1.2.2).

In this series of experiment, the granularity of the optical power difference was refined to 1 dB increments. This allows a better accuracy when determining the threshold optical power difference that will impact CUT performance. The CUT BER was set to 10^{-9}. As the optical power of the nearest-neighbor channels is increased in 1 dB increments using manual optical attenuators and relative to the CUT optical power, variations in BER are observed. The "threshold optical power difference" between the CUT and the nearest-neighbor channels is somewhere between 3 and 4 dB difference for all channels measured. Further degradation in CUT BER is observed as the optical power difference is increased further. Results are shown in Table 14 below. Because throughout the experiment, the POI components were found to perform uniformly under normal operation, it is assumed in confidence that it will be the case in this particular experiment as well. This allows a reduction in the total number of channels to test. In this particular experiment a random selection of array elements was done instead of a full experimental characterization to reduce testing time.

	BER					
Optical Power Δ (dB)	**Channel 1**	**Channel 3**	**Channel 4**	**Channel 6**	**Channel 9**	**Channel 10**
3 dB	2.63 E-9	3.87E-10	10E-10	1.56 E –9	10-10	9.48E-9
4 dB	2.11E-7	4.71E-6	0.43 E-7	2.10E-7	1.78E-7	6.25E-7
5 dB	9.43E-5	5.69E-5	1.23 E-5	6.5 E-5	4.66-5	8.44E-4

Table 14: BER variation in the CUT with differences in optical power in the aggressor channels

Referring back to Table 13, with 3dB as the threshold optical power difference, the power penalty improvement will then be 1.5 dB approximately, so that the 5.8 dB worst-case power penalty found in section 6.1.1.4 can then be adjusted to 4.3 dB. A 2-3 dB difference in optical power can translate to a 3.5 dB to 5.8 dB power penalty as observed in Figure 25. This penalty can be significant when compared to the 12.5 dBm optical link budget found in [1]. A quick verification of the link budget for all channels again demonstrates uniformity across the array for both the initial link budget and the link budget adjusted with the 1.5 dB improvement: the average adjusted link budget for all channels listed in Table 15 is 12.48 dB with a standard deviation of 0.73 dB, with a worst-case of 11.3 dB. Thus the impact of the power penalty due to multi-channel operation will also be consistent across the array. A bit rate increase from 2.5 Gb/s to 3.125 Gb/s would de-rate the link budgets by an additional 0.3 dB to complete worst-case analysis.

Channel	1	2	3	4	5	6	7	8	9	10	11	12
Initial Link Budget (dB)	12.65	10.95	11.5	10.7	10.9	10.25	9.8	11.15	10.6	10.5	11.3	11.45
Adjusted Link Budget	14.15	12.45	13.0	12.2	12.4	11.75	11.3	12.65	12.1	12.0	12.8	12.95

Table 15: Link budget per POI channel (multi-channel operation at 2.5 Gb/s)

In real-life point-to-point or single-hop applications using the present POI, a channel will rarely be attenuated by more than 3 dB relative to the other channels in the array (referring to the Rx sensitivities of the channels shown in Table 9). However, when used in multi-hop O-MINs with optical redirection boxes, one channel can go through many redirection boxes and thus be attenuated by more than 3 dB relative to other channels not going through as many redirection boxes (as shown previously in Figure 4). The above limitation will have to be taken into account when determining the link budget for all the fiber links used in an O-MIN: a limit on the number of redirection boxes that can be connected together will be imposed as the total sum of the losses attributed to these boxes cannot be greater than 3 dB without impacting the link BER or power budget. Assuming a 1 dB loss per redirection box, 3 redirection boxes is a good approximation of the maximum number of redirection boxes that can be interconnected optically in a row to create an O-MIN. The limitations can also be applied to the maximum number of hops an optical signal can go through if more than 3 optical redirection boxes are used. This last approach however will require some form of optical signal management.

6.1.2.4 Impact of cross talk on POI jitter performance uniformity across the array

A fairly extensive jitter analysis was done in [1]. In this present thesis, the tolerance of the POI to multi-channel induced jitter and its uniformity of the jitter across the array are of interest.

The worst -case eye opening of 44.8% at –14 dBm for channel 6 shown in Figure 31 and Table 16 is still large enough to meet the system link budget determined [1]. The corresponding eye diagram is shown in Figure 32. Multi-channel operation of the POI will degrade the channel jitter performance. However, this performance is still acceptable within the jitter budget defined for a POI used in the scalable router application defined in this thesis. In other words, the POI studied in this thesis exhibits high tolerance to jitter since the 20% jitter performance degradation is acceptable in the context of point-to-point links in an O-MIN application. Further study will be needed to determine the jitter tolerance for multi-hop applications.

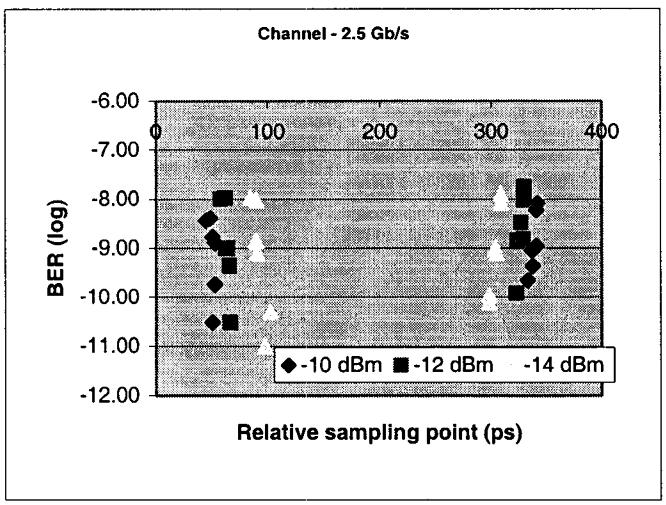

Figure 31: Bathtub curve for channel #6 (2.5 Gb/s at 204 m.)

2.5 Gbps		Eye opening (Average)	
BER(log)	-10 dBm	-12 dBm	-14 dBm
-1	92.9%	82.9%	75.2%
-2	90.3%	80.7%	72.4%
-3	87.7%	78.5%	69.6%
-4	85.2%	76.3%	66.9%
-5	82.6%	74.1%	64.1%
-6	80.0%	71.9%	61.3%
-7	77.4%	69.8%	58.6%
-8	74.8%	67.6%	55.8%
-9	72.2%	65.4%	53.0%
-10	69.7%	63.2%	50.3%
-11	67.1%	61.0%	47.5%
-12	**64.5%**	**58.8%**	**44.8%**
-13	61.9%	56.7%	42.0%
-14	59.3%	54.5%	39.2%
-15	56.7%	52.3%	36.5%

Table 16: Channel #6 eye opening (2.5 Gb/s at 204 m.)

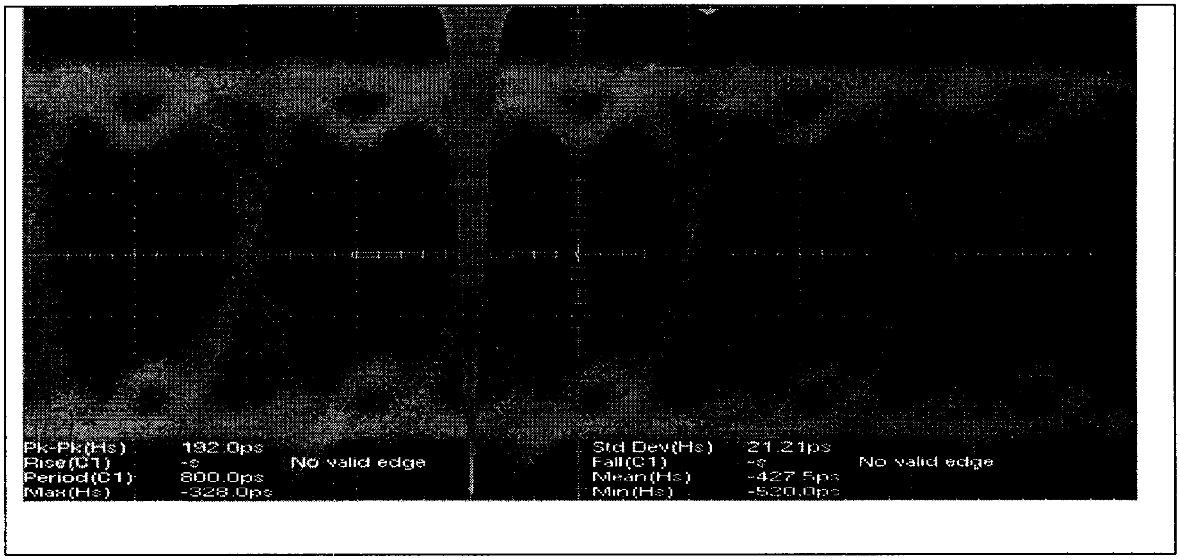

Figure 32: Eye diagram results for jitter measurements (channel #6 at 2.5 Gb/s, 204 m @ -12 dBm Rx power)

6.2 Summary

The tests described in Chapter 5 were carried out completely, and in some cases additional testing was performed. Optical power measurements, Rx sensitivity measurements, and various jitter measurements were performed to successfully characterize the power and jitter penalties due to multi-channel operation of the POI. This testing confirmed that the POI selected in this paper could be used in an O-MIN architecture. It also demonstrated that the crosstalk-induced power and jitter penalties are mostly occurring at the Rx end of the POI. With the results obtained, it was possible to adjust the optical power budgets of the O-MIN system. Finally, the methodology followed in this chapter can be applied when testing any other POI components that will be used in an O-MIN architecture.

6.3 References

1. M. Salzberg, "Testing and Characterization of a Parallel Optical Interconnect for a Scalable Routing System" Master's thesis, McGill University, 2001.

Chapter 7 Conclusion and Future Work

In this thesis, much work has been completed to characterize the crosstalk of a parallel optical interconnect used in optical multi-stage networks. A brief review of this work is provided in this final chapter. Future testing activities to improve the crosstalk characterization of POI technology are also considered.

7.1 Review

To meet the ever-growing bandwidth demands of IP networks, new scalable routers are emerging based on multi-stage architectures. These consist in creating a single system by interconnecting multiple shelves together. Parallel optical technologies have been shown to be the most effective method to interconnect shelves in a multi-stage system. With the use of optical redirection boxes, the total number of optical links needed is reduced. Systems using a combination of optical redirection boxes and POI links are called optical multi-stage interconnect networks or O-MINs.

Today, POI technology is available to support multi-stage scalable router applications and offers many advantages over other optical technologies available today. The components selected in this thesis were state-of-the-art components. Their key characteristics relevant to the subsequent crosstalk evaluation testing were presented as well.

By studying the characteristics of the POI components, it is possible to find out about their crosstalk properties. The key attributes needed to minimize electrical and optical crosstalk in the POI at both the Tx and Rx ends have been determined in Chapter 3. In summary, they are:

1. Oxide-confined MQW VCSELs
2. PIN photodiodes
3. Minimum optical coupling distance
4. Very short traces between active components and driver components
5. Shielded signal traces
6. Differential signaling scheme

7. Temperature compensating structure and/or circuits

The effects of thermal variations in the POI components on performance have not been studied in this thesis. A brief overview of thermal effects and the solutions to minimize these has been provided for completeness.

Optical and electrical inter-channel crosstalk within the parallel optical interconnect components (at the Tx and Rx side of the POI) can degrade the interconnect performance. The key performance parameters that need to be evaluated are bit error rate (BER), jitter as well as uniformity across the array. Uniformity is of particular importance in an O-MIN since it simplifies system link budgeting. Although [1] provided a very thorough analysis of the POI used in this thesis, it did not include in-depth testing under multi-channel operation. The performance degradation found in this thesis is really evaluated under multi-channel operation, which represents a real-life operating condition of the POI.

In order to characterize the electrical and optical crosstalk of the POI components and verify they meet the design specifications, several unique test set-ups were created and a detailed test plan was developed and executed.

The test plan was implemented with slight modifications for improved accuracy. It was found that only the nearest-neighbour channels affected the CUT performance in the POI tested. Multi-channel operation of the POI does induce a power penalty of as high as 5.8 dB relative to single channel operation and the maximum variation across the array is 2.85 dB. This initial measurement technique did not represent real-life operational situations however. The power penalty was therefore adjusted by 1.5 dB using further experimental results to get a worst-case link budget of 11.3 dB, which more closely matched real-life usage of the POI. 2.5-3 dB was found to be the threshold optical power difference between adjacent channels and the CUT, which corresponds roughly to a 3 or 4 hops O-MIN, depending on the insertion losses of the optical redirection box. Crosstalk was shown to only occur at the receive end of this particular POI, which means that there will be no Tx-induced crosstalk at the optical redirection box. Only the inherent crosstalk components of the optical redirection box and the receive end of the POI will affect the performance of the POI used in an O-MIN. Calculations showed that there is no optical crosstalk due to inefficient coupling at the receive end of this particular POI.

The POI tested was also found to be jitter-tolerant as the worst-case jitter penalty under multi-channel operation still was twice the jitter budget specified in [1]. This provides very large jitter margins and thus the POI tested in this thesis is jitter tolerant. This margin is sufficient for point-to-point optical interconnect links but still needs to be verified for multi-hop O-MINs.

Because the POI tested was made of prototype components, recommendations were made to the component supplier for further POI performance improvements.

Finally, the techniques used in this thesis can be applied to measure the performance degradation of other types of POI.

7.2 Future Work

Further investigations are required in order to fully characterize the crosstalk-induced performance degradation of the parallel optical interconnect.

The most important work that needs to be performed next is to determine the impact of optical redirection boxes on the jitter performance of multi-hop POI-linked O-MINs. Although the POI was found to be jitter tolerant in point-to-point links in this thesis, studies with multi-hop O-MINs need to be completed. Such testing would determine the nature of the optical crosstalk (homodyne or heterodyne, coherent or incoherent) at the RB as well as its impact on system performance.

Further characterization of the Rx crosstalk is also needed in order to better understand the cause of the crosstalk induced power penalty. With BGA-based POI components, it is difficult to determine but with other pin-based or lead-based components, this can be done. This work can provide further direction to the component manufacturer for improvements.

Observing the effects of long-term operation on crosstalk performance also needs to be completed. For carrier-class system operation, it is important to verify that the POI performance will remain stable over long periods of time (> 10 years).

It will be interesting to use the crosstalk measurements techniques developed in this thesis to test new POI technology, like 2-D VCSEL/PIN array based technology or CWDM VCSEL based technology. These new technologies will be used to provide cost-efficient high-bandwidth interconnect capacity that will be needed in next-generation multi-stage scalable routers.

POI technology not only offers immediate advantages for routers requiring high-bandwidth, cost-effective interconnect technology but it is the only technology enabling dramatic improvement in scalability. As routers scale further to meet the tremendous bandwidth growth demand fuelled by Internet, POI technology will become more prevalent in the system interconnects. This highlights the value in testing and characterizing POI components today and tomorrow.

7.3 References

1. M. Salzberg, "Testing and Characterization of a Parallel Optical Interconnect for a Scalable Routing System" Master's thesis, McGill University, 2001.